

1 **Genomic variants among threatened *Acropora* corals**

2

3 **Authors:** S. A. Kitchen^{*†}, A. Ratan^{*‡}, O.C. Bedoya-Reina^{§**}, R. Burhans^{††}, N. D. Fogarty^{‡‡}, W.
4 Miller^{††}, I. B. Baums^{†§§}

5 * Authors contributed equally to the manuscript

6 **Author Affiliations:**

7 † 208 Mueller Lab, Biology Department, The Pennsylvania State University, University Park PA
8 16802 sak89@psu.edu, baums@psu.edu

9 ‡ Department of Public Health Sciences and Center for Public Health Genomics, University of
10 Virginia, Charlottesville VA 22908 ratan@virginia.edu

11 § MRC Functional Genomics Unit, Department of Physiology, Anatomy and Genetics,
12 University of Oxford, South Parks Road, Oxford OX1 3PT, UK oscar@bx.psu.edu

13 ** MRC Human Genetics Unit, MRC Institute of Genetics and Molecular Medicine, The
14 University of Edinburgh, Western General Hospital, Crewe Road, Edinburgh, UK.

15 †† Centre for Comparative Genomics and Bioinformatics, Pennsylvania State University,
16 University Park, PA 16802, USA rico@bx.psu.edu, webb@bx.psu.edu

17 ‡‡ Department of Marine and Environmental Sciences, Nova Southeastern University, Fort
18 Lauderdale, FL 33314, Nicole.fogarty@nova.edu

19

20 **Data Accession numbers:** NCBI SRA accession numbers are SRR7235977-SRR7236038.

21

22 **Running Title:** Genomic variants among threatened corals

23

24 **Keywords:** coral, Caribbean, single nucleotide polymorphism, population genomics, Galaxy

25

26 **Corresponding Author (§§):** I.B Baums, 208 Mueller Lab, Biology Department, The

27 Pennsylvania State University, University Park PA 16802, Fax +1 814 865 9131,

28 baums@psu.edu

29

30 **Article Summary**

31 We provide the first comprehensive genomic resources for two threatened Caribbean reef-
32 building corals in the genus *Acropora*. We identified genetic differences in key pathways and
33 genes known to be important in the animals' response to the environmental disturbances and
34 larval development. We further provide a list of candidate loci for large scale genotyping of these
35 species to gather intra- and interspecies differences between *A. cervicornis* and *A. palmata* across
36 their geographic range. All analyses and workflows are made available and can be used as a
37 resource to not only analyze these corals but other non-model organisms.

38

39 **ABSTRACT**

40 Genomic sequence data for non-model organisms are increasingly available requiring the
41 development of efficient and reproducible workflows. Here, we develop the first genomic
42 resources and reproducible workflows for two threatened members of the reef-building coral
43 genus *Acropora*. We generated genomic sequence data from multiple samples of the Caribbean
44 *A. cervicornis* (staghorn coral) and *A. palmata* (elkhorn coral), and predicted millions of
45 nucleotide variants among these two species and the Pacific *A. digitifera*. A subset of predicted
46 nucleotide variants were verified using restriction length polymorphism assays and proved useful
47 in distinguishing the two Caribbean Acroporids and the hybrid they form ("*A. prolifera*").
48 Nucleotide variants are freely available from the Galaxy server (usegalaxy.org), and can be
49 analyzed there with computational tools and stored workflows that require only an internet
50 browser. We describe these data and some of the analysis tools, concentrating on fixed
51 differences between *A. cervicornis* and *A. palmata*. In particular, we found that fixed amino acid
52 differences between these two species were enriched in proteins associated with development,
53 cellular stress response and the host's interactions with associated microbes, for instance in the
54 Wnt pathway, ABC transporters and superoxide dismutase. Identified candidate genes may
55 underlie functional differences in the way these threatened species respond to changing
56 environments. Users can expand the presented analyses easily by adding genomic data from
57 additional species as they become available.

58 INTRODUCTION

59 Genomic data for non-model organisms are becoming available at an unprecedented rate.
60 Analyses of these data will advance our understanding of the capacity of organisms to adapt,
61 acclimatize or shift their ranges in response to rapid environmental change (Savolainen *et al.*
62 2013). While genome sequencing itself has become routine, bioinformatics treatment of the data
63 still presents hurdles to the efficient and reproducible use of this data (Nekrutenko and Taylor
64 2012). Thus, genomic variant analysis workflows (e.g. Bedoya-Reina *et al.* (2013) are needed to
65 eliminate some of these computational hurdles and increase reproducibility of analyses. Here, we
66 develop such tools, apply them to threatened reef-building corals and present novel findings with
67 respect to the molecular pathways used by these species to respond to environmental stimuli.

68 The *Acropora* species, *A. cervicornis* and *A. palmata* were the main reef-building corals of
69 the Caribbean (Figure 1). These corals have greatly decreased in abundance during recent years
70 due to infectious disease outbreaks, habitat degradation, storm damage, coral bleaching,
71 outbreaks of predators and anthropogenic activities (Bruckner 2002). A large body of previous
72 studies has investigated the effects of environmental stress in Caribbean Acroporid corals
73 (Randall & Szmant 2009; DeSalvo *et al.* 2010; Baums *et al.* 2013; Libro *et al.* 2013; Polato *et al.*
74 2013; Parkinson *et al.* 2015). These studies highlight changes in the molecular, cellular, and
75 physiological response of these species to an unprecedented elevation in seawater temperature.
76 Increases in water temperature of only 2 -3 °C can reduce the fertilization rates, reduce larval
77 survival, and deplete genotypic diversity of Caribbean Acroporids (Randall & Szmant 2009;
78 Williams & Miller 2012; Baums *et al.* 2013).

79 Because of a tremendous die-off, both species are now listed as threatened on the United
80 States Federal Endangered Species List (Anonymous 2006). Extensive conservation efforts are
81 currently underway across the range, which will be considerably facilitated by the acquisition of
82 genomic data. For instance, these data will help to identify management units, evolutionary
83 significant units, hybridization dynamics, genotypic diversity cold-spots and interactions with the
84 corals' obligate symbionts in the genus *Symbiodinium* (Baums 2008; van Oppen et al. 2015). The
85 project described here represents an early effort to move beyond low-resolution sequencing and
86 microsatellite studies (Vollmer & Palumbi 2007; Baums *et al.* 2014) and employ the power of
87 full-genome analysis (Drury et al. 2016).

88 Here, we present genome-wide single nucleotide variants (SNVs) between the two
89 Caribbean Acroporids relying on the genome assembly for a closely related species, *A. digitifera*
90 (Shinzato et al. 2011) (Figure 1). We have successfully used the same approach to analyze
91 genomes using much more distant reference species, such as polar, brown and black bears based
92 on the dog genome (Miller *et al.* 2012), and giraffe based on cow and dog (Agaba et al. 2016).
93 We highlight several examples of how these SNVs enable population genomic and evolutionary
94 analyses of two reef-building coral species. The SNV results are available on the open source,
95 public server Galaxy (Afgan et al. 2016), along with executable histories of the computational
96 tools and their settings. This workflow presented here for corals and by Bedoya-Reina et al.
97 (2013) can be transferred for genomic analyses of other non-model organisms, and provide
98 abundant information in a reproducible manner.

99 MATERIALS AND METHODS

100 DNA Extraction and Sequencing

101 For each species, five previously genotyped samples from the Baums Lab coral tissue
102 collection were selected from each of the four sites representing their geographic range: Florida
103 (FL), Belize (BE), Curacao (CU) and U.S. Virgin Islands (VI; Table 1) (Baums et al. 2009;
104 Baums et al. 2005). An additional sample for each species from Florida (*A. cervicornis*
105 CFL14120 and *A. palmata* PFL1012) was selected for deep genome sequencing because they are
106 located at easily accessible and protected sites in the Florida Keys (*A. palmata* at Horseshoe Reef
107 and *A. cervicornis* at the Coral Restoration Foundation nursery), and are predictable spawners
108 that are highly fecund. High molecular weight DNA was isolated from each sample using the
109 Qiagen DNeasy kit (Qiagen, Valencia, CA) according to the manufacturer's protocol. DNA
110 quality and quantity was assessed with gel electrophoresis and Qubit 2.0 fluorometry (Thermo
111 Fisher, Waltham, MA), respectively. Sequence library construction and sequencing was
112 completed by the Pennsylvania State University Genomics Core Facility. Paired-end short insert
113 (550 nt) sequencing libraries of the two deeply sequenced genomes were constructed with 1.8-2
114 μ g sample DNA and the TruSeq DNA PCR-Free kit (Illumina, San Diego, CA). The remaining
115 40 paired-end short insert (350 nt) sequencing libraries (Table S1) were constructed using 100 ng
116 sample DNA and the TruSeq DNA Nano kit (Illumina, San Diego, CA). Deep- and shallow-
117 sequence libraries were pooled separately and sequenced on the Illumina HiSeq 2500 Rapid Run
118 (Illumina, San Diego, CA) over two lanes and four lanes, respectively.

119 ***A. digitifera* Assembly and Inter-species Gene Model Comparisons**

120 We downloaded the *A. digitifera* genome assembly and GFF-formatted gene annotations
121 from NCBI GCA_000222465.2 Adig_1.1). To conduct the pathway enrichment analysis, we
122 obtained additional annotation from the Kyoto Encyclopedia of Genes and Genomes (KEGG)
123 (Kanehisa et al. 2017). During gene prediction, gene annotation can be error prone and misled by
124 assembly gaps or errors, imprecision of *de novo* gene predictors and/or errors in gene annotations
125 in the species used for comparison, among other sources. To overcome these known issues, our
126 approach included, at a minimum, submitting the putative amino acid sequence to the blastp
127 server maintained by the Reef Genomics Organization (Liew et al. 2016) () and the blastp and/or
128 psi-blast servers at NCBI (Altschul et al. 1997) (). We also used the Reef Genomics website to
129 assess the degree of inter-species sequence conservation among 20 corals in Figure 1 (resources
130 include transcriptomes and genomes, details provided in Bhattacharya et al. (2016), and the
131 Genome Browser () at the University of California at Santa Cruz (Kent et al. 2002) to measure
132 the inter-species conservation of the orthologous mammalian residue. We interpret the degree of
133 conservation at a protein position and its immediate neighbors as suggesting the amount of
134 selective pressure and the functional importance of the site.

135 **Single Nucleotide Variant and Indel Calls**

136 We aligned the paired-end sequences for the 42 samples to the *A. digitifera* reference
137 genome sequence using BWA version 0.7.12 (Li and Durbin 2009) with default parameters. On
138 average, we were able to align ~89% of the reads for each individual, and ~74% of the reads
139 aligned with a mapping quality > 0. Paired-end reads are generated by sequencing from both
140 ends of the DNA fragments, and we found that about 70% of these reads aligned within the

141 expected distance from its mate in those alignments (see Table S1 for details). We used
142 SAMBLASTER version 0.1.22 (Faust and Hall 2014) to flag potential PCR duplicate reads that
143 could otherwise affect the quality of the variant calls (Table S1). Considering data from all
144 individuals simultaneously, we used SAMtools version 1.3.1 (Li et al. 2009) to identify the
145 locations of putative variants with parameters `-g` to compute genotype likelihoods, `-A` to include
146 all read pairs in variant calling, and `-E` to recalculate the base alignment quality score against the
147 reference *A. digitifera* genome. Variants were called with bcftools version 1.2 (Li 2011)
148 multiallelic caller and further filtered to keep those variants for which the total coverage in the
149 samples was less than 1,200 reads (to limit the erroneous calling of variant positions in repetitive
150 or duplicated regions), the average mapping quality was greater than 30, and the fraction of reads
151 that aligned with a zero mapping quality was less than 0.05. The VCF file of nucleotide variants
152 was converted to `gd_snp` format using the “Convert” tool from the “Genome Diversity”
153 repository on Galaxy, after separating the substitution and insertion/deletion (indel) variants. The
154 resulting sets of SNVs and indels are available on Galaxy (*a permanent link will be made*
155 *available upon acceptance*). The mitochondrial variants were similarly identified using
156 the *A. digitifera* mitochondrial reference genome (GenBank: NC_022830), and Figure S3 was
157 drawn using Millerplot (<https://github.com/aakrosh/Millerplot>).

158

159 The Galaxy tool “Phylogenetic Tree” under Genome Diversity (Bedoya-Reina et al. 2013)
160 was used to calculate the genetic distance between two individuals at a given SNV as the
161 difference in the number of occurrences of the first allele. For instance, if the two genotypes are
162 2 and 1, i.e., the samples are estimated to have respectively 2 and 1 occurrences of the first allele
163 at this location, then the distance is 1 (the absolute value of the difference of the two numbers).

164 The Neighbor-joining tree was constructed with QuickTree (Howe et al. 2002) and visualized
165 with draw_tree utility script in package PHAST (Hubisz et al. 2010). We used I-TASSER online
166 server for protein structure prediction (Yang et al. 2015) to model and further help to develop
167 hypotheses about functionality of several mutations in STE20-related kinase adapter protein
168 alpha protein (NCBI: LOC107340566). Identification of enriched KEGG pathways was
169 completed using the “Rank Pathways” tool, which compares the gene set with SNVs against the
170 complete set of genes in the pathway using the statistical Fisher’s exact test.

171 **Genomic Regions of Differentiation**

172 We assigned a measure of allele frequency difference to each SNV analogous to calculations
173 of F_{ST} for intra-species comparisons using the “Remarkable Intervals” Galaxy tool (score shift
174 set to 90%). F_{ST} values can be used to find genomic regions where the two species have allele
175 frequencies that are remarkably different over a given window or interval, i.e., the F_{ST} s are
176 unusually high. Such intervals may indicate the location of a past "selective sweep" (Akey et al.
177 2002) caused by a random mutation that introduces an advantageous allele, which rises to
178 prominence in the species because of selective pressures, thereby increasing the frequency of
179 nearby variants and changing allele frequencies from those in an initially similar species. In
180 theory, the F_{ST} ranges between 0, when the allele frequencies are identical in the two species, to
181 1, for a fixed difference. However, in practice it works better to use an estimation formula that
182 accounts for the limited allele sampling; we employ the “unbiased estimator” of Reich et al.
183 (2009), because it performs best on the kinds of data used here, according to Willing *et al.*
184 (2012). It should be noted that care must be taken when interpreting high F_{ST} values this way,
185 since they can also be caused by genetic drift, demographic effects, or admixture (Holsinger and

186 Weir 2009). We compared these intervals to the genome-wide F_{ST} estimate calculated using the
187 Galaxy tool “Overall FST”.

188 **PCR-Ready SNV Markers and RFLP Validation**

189 PCR-ready SNVs were identified based on the following criteria: 1) the SNV-caller
190 considered them to be high-quality (Phred-scaled quality score ≥ 900), 2) all 21 *A. cervicornis*
191 samples looked homozygous for one allele while all 21 *A. palmata* samples looked homozygous
192 for the other allele and 3) there were no observed SNVs, indels, low-complexity DNA or
193 unassembled regions within 50 bp on either side of the SNV.

194 From the PCR-ready SNVs, we developed a PCR-restriction fragment length polymorphism
195 (RFLP) assay to validate a subset of fixed SNVs with additional Caribbean Acroporids samples,
196 including the hybrid of the two species, *Acropora prolifera* (Table S2). We screened 197 fixed
197 SNVs with 50bp flanking sequence (101bp total) using the webserver SNP-RFLPing2 (Chang et
198 al. 2006; Chang et al. 2010) to find a set of loci that would cut with common restriction enzymes
199 (*HaeIII*, *DpnII*, *Hinfl*, *EcoRV*, and *HpyCH4IV* all from New England Biolabs, Ipswich, MA).
200 Eight loci were selected, of which half cut *A. palmata*-like SNVs while the other half cut *A.*
201 *cervicornis*-like SNVs (Table S3). For each diagnostic locus, additional flanking sequence was
202 extracted from the scaffold until another restriction enzyme recognition site was encountered for
203 that specific locus-restriction enzyme combination. Primers were designed for the extended
204 flanking sequence using Primer3web version 4.1.0 (Untergasser et al. 2012).

205 A reference set of parental ($n= 10$ *A. palmata* and $n= 9$ *A. cervicornis*) and hybrid ($n = 27$
206 colonies) samples from across the geographic range were tested with a previously developed
207 microsatellite assay based on five markers (Baums et al. 2005) and the RFLP assay (Table S2). A

208 test set of hybrids ($n=20$ colonies) that did not have previous genetic information was also
209 included to compare taxon assignment between the two marker sets. Hybrids were initially
210 identified in the field based on intermediate morphological features following Cairns (1982);
211 Van Oppen *et al.* (2000); Vollmer and Palumbi (2002) .

212 For all samples, DNA was extracted using the DNeasy kit (Qiagen, Valencia, CA). PCR
213 reactions consisted of 1X NH₄ Buffer (Bioline, Boston, MA), 3 mM MgCl₂ (Bioline, Boston,
214 MA), 1 mM dNTP (Bioline, Boston, MA), 250 nmol forward and reverse primers (IDT,
215 Coralville, Iowa), 1 unit of Biolase DNA polymerase (Bioline, Boston, MA) and 1 μ l of DNA
216 template for a total volume of 10 μ l. The profile for the PCR run was as follows: 94 °C for 4 min
217 for initial denaturing, followed by 35 cycles of 94 °C for 20s, 55 °C for 20s, and 72 °C for 30s,
218 and a final extension at 72 °C for 30min. For each locus, 5 μ l of PCR product was combined
219 with 1X restriction enzyme buffer (New England Biolabs, Ipswich, MA) and 0.2 μ l restriction
220 enzyme (New England Biolabs, Ipswich, MA) for a total reaction volume of 10 μ l and incubated
221 according to the manufacturer's recommendation. PCR and digest fragment products were
222 resolved by 2% TAE agarose gel electrophoresis at 100 V for 35 min, except for locus
223 NW_015441368.1: 282878 that was run on 3.5% TAE agarose gel at 75 V for 45 min to resolve
224 the smaller fragments. Banding patterns were scored for each locus as homozygous for either
225 parent species (1 or 2 bands) or heterozygous (3 bands).

226 Reference samples were first assigned to taxonomic groups (*A. palmata*, *A. cervicornis* , F1
227 or later generation hybrid) based on allele frequencies at five microsatellite loci (Baums *et al.*
228 2005) by NEWHYBRIDS (Anderson and Thompson 2002). A discriminant factorial
229 correspondence analysis (DFCA) was performed on the microsatellite and SNV marker data
230 separately to predict sample membership to the taxonomic groups: *A. palmata*, *A. cervicornis*, F1

231 hybrid or later generation hybrid. The FCA performed in GENETIX version 4.05 (Belkhir et al.
232 2004) clustered the individuals in multi-dimensional space based on their alleles for each marker
233 type. The factorial axes reveal the variability in the data set with the first factor being the
234 combination of alleles that accounts for the largest amount of variability. The FCA scores for all
235 axes were used in a two-step discriminant analysis using the R statistical software (RCoreTeam
236 2017) to calculate the group centroid, or mean discriminant score for a given group, and
237 individual probability of membership to a given group using leave-one-out cross-validation. First,
238 the parameter estimates for the discriminant function of each group were trained by the FCA
239 scores from the reference samples. Second, those functions were used to assign all samples,
240 including the test set of hybrids, based on their FCA scores to a taxon group.

241 **Data Availability**

242 The executable histories for the SNV and protein analyses and their respective data sets are
243 available on Galaxy (link provided in final publication). Table 2 lists the data sets available
244 on Galaxy. Specifically, the data sets “coral snps” and “intra-codon variants” are tables of
245 variants with positions in reference to the *A. digitifera* genome. The data set “PCR-Ready SNVs”
246 are 101 bp sequences extracted from the *A. digitifera* genome, with 50 bp flanking sequence
247 surrounding the fixed SNV. Raw sequence data are deposited in the NCBI Sequence Read
248 Archive (accessions SRR7235977-SRR7236038).

249 **RESULTS**

250 **Variants between Three Acroporid Species**

251 For each species, we performed deep-coverage sequencing (roughly 150-fold coverage) of
252 one sample and shallow sequencing (roughly 5-fold to 10-fold) of 20 samples, five each from
253 four geographic locations (Florida, the Virgin Islands, Belize, and Curacao) (Figure 2A). For
254 details, see Table 1. The sequence coverage distribution for the Acroporid samples was
255 comparable between species (*A. cervicornis*: Figure S1 and *A. palmata*: “coral SNPs” history at
256 [link to be provided in final publication](#)).

257 Rather than relying on *de novo* assembly and gene annotation of our data, we based the
258 analysis reported below on an assembly and annotation of the highly similar reference genome of
259 *A. digitifera* (NCBI: GCA_000222465.2 Adig_1.1) (Shinzato *et al.* 2011). This strategy increases
260 reproducibility and leverages the work of large and experienced bioinformatics groups.
261 Important advantages of using this third species is that we can transfer its gene annotation as well
262 as “polarize” variants, as follows. The two sequenced species in this study diverged in the
263 Eocene about 34.2 mya from the most recent common ancestor they share with the reference
264 species *A. digitifera* (Figure 1) (van Oppen *et al.* 2001; Richards *et al.* 2013). Thus, with a
265 difference observed among the *A. cervicornis* and *A. palmata* samples, the allele agreeing with *A.*
266 *digitifera* can be interpreted as ancestral, and the variant allele as derived.

267 We identified both substitution and indel variants by aligning our paired-end sequencing
268 reads to the *A. digitifera* assembly and noting nucleotide differences with *A. cervicornis* and *A.*
269 *palmata* (Table 2). Specifically, each reported substitution variant is a position in an *A. digitifera*
270 assembly scaffold where at least one of our sequenced samples has a nucleotide that is different

271 from the *A. digitifera* reference nucleotide, after all the thresholds on read-depth and mapping
272 quality as discussed in the Methods were applied. We call each of these an SNV (single-
273 nucleotide variant) because “SNP” (single-nucleotide polymorphism) is commonly used to
274 describe an intra-species polymorphism. These data permit comparisons among the three
275 *Acropora* species, although this paper focuses on *A. cervicornis* and *A. palmata*, and ignores
276 unanimous differences of the new sequences from the reference.

277 **Fixed differences of SNVs and Indels between *A. cervicornis* and *A. palmata***

278 Single nucleotide variants and indels can be used to explore either intra- or inter-species
279 variation, using similar techniques in both cases. Of the 8,368,985 SNVs, 4,998,005 are
280 identically fixed in *A. cervicornis* and *A. palmata*, leaving 3,370,980 variable within our two
281 sequenced species, only 1,692,739 of which were considered high-quality (Phred-scaled quality
282 ≥ 900 , Table 2). The results reported below use this set of substitution variants. A phylogenetic
283 tree based on the genetic distance between those SNVs clearly separates the two species, and
284 distinguishes the samples from each species according to where they were collected in most
285 cases (Figure S2). The same is true of a Principal Component Analysis (Figure 2). From all the
286 SNVs, both synonymous and non-synonymous amino acid substitutions were identified from the
287 coding sequences (Table 2). Out of the 561,015 putative protein-coding SNVs, we retained the
288 120,206 deemed “high quality” and variable in the two newly sequenced species. To complete
289 our analysis, we identified 172 mitochondrial SNVs, which are highly concentrated in the gene-
290 free “control region” (Figure S3). This region also contains the only identified indel between *A.*
291 *digitifera* and the two Caribbean Acroporids (Figure S3).

292 The examples in most of the following sections investigate only inter-species differences,
293 and in particular focus on fixed SNVs, i.e., locations where the 21 sequenced *A. cervicornis*
294 samples share the same nucleotide and the 21 *A. palmata* samples share a different nucleotide.
295 Variants were filtered so that the genotype of each shallow genome within a species would
296 match its deeply sequenced genome. This approach identified 65,533 fixed nucleotide SNV
297 differences and 3,256 fixed amino acid differences, spread across 1,386 genes (Table 2, see
298 Galaxy histories “coral SNPs” and “coral proteins”). These SNVs are potentially useful for
299 investigating the genetic causes of phenotypic differences between the two *Acropora* species. In
300 the following, by “fixed” difference we always mean fixed between *A. cervicornis* and *A.*
301 *palmata*. It should be also be noted that such variants may be simply the result of demographic
302 process rather than the result of adaptation to different niches.

303 Identified indels can also be analyzed to understand genomic difference between the studied
304 species. Filtered in a manner analogous to the SNVs (requiring “high quality” and variability in
305 *A. cervicornis* plus *A. palmata*), the original set of 940,345 genome-wide indels (Table 2) was
306 reduced to 149,036. Of those, 2,031 were identified as fixed between *A. cervicornis* and *A.*
307 *palmata*. They provide an additional set of hints for tracking down the genetic underpinnings of
308 inter-species phenotypic differences, since indels are often more disruptive than substitutions.

309 **Examples of Substitutions with Potential Protein Modifications**

310 We scanned the list of proteins with a fixed amino acid difference (or several fixed
311 differences) to examine more closely. One potentially interesting fixed amino acid substitution is
312 found in superoxide dismutase (SOD), whose activity is essential for almost any organism, and
313 particularly for corals, like *Acropora*, that harbor symbionts of the genus *Symbiodinium*. This

314 fixed difference was identified in comparison to *A. digitifera* (NCBI: LOC107335510 or Reef
315 Genomic: *Acropora_digitifera_12779*), which strongly matched (E-value 3e-85) the human
316 manganese SOD mitochondrial protein (GenBank: NP_001309746.1; Figure S4). We observed a
317 glutamate (E) to glutamine (Q) substitution in *A. cervicornis*, corresponding to position 2 of the
318 *A. digitifera* orthologue (Figure S4). According to the surveyed coral sequences, the Q is fixed in
319 a number of other corals, except for an E shared by *A. digitifera*, *A. palmata*, *A. hyacinthus*, *A.*
320 *millepora* and *A. tenuis* suggesting a lineage-specific mutation (Figure S4).

321 Another gene, NF-kappa-B inhibitor-interacting Ras-like protein 2 (NKIRAS2; NCBI:
322 LOC107355568 and Reef Genomics: *Acropora_digitifera_6635*) has two putative fixed amino
323 acid difference in the Caribbean Acroporids (Figure S5). One, an E to aspartic acid (D)
324 substitution, occurs in the middle of a “motif” LGTERGV→LGTD~~R~~GV that is fairly well
325 conserved between *A. palmata* and other members of the complex corals including *Porites* spp.
326 and *Astreopora* sp. as well as robust corals except the Pocilloporidae family (*S. pistillata* and
327 *Seriatopora* spp.), but not with *A. cervicornis* or other Acroporids (Figure S5). Thus, this appears
328 to be a recurrent substitution in corals. The second putative fixed amino acid difference in this
329 gene is unique to *A. cervicornis* from the corals we surveyed. The transition is from a polar but
330 uncharged asparagine (N) to a positively charged lysine (K) in the short motif
331 SVDGSNG→SVDGSKG (Figure S5). This substitution might have consequences on the tertiary
332 structure and function of this gene in *A. cervicornis* compared to the other Acroporids.

333 **Fixed Indels in Protein-Coding Regions**

334 We also looked for fixed indels in protein-coding regions among corals compared to
335 respective mammalian orthologues. Of the 2,031 fixed indels identified, most were not found in

336 coding sequence with only 18 genes having a fixed indel. For closer inspection, we picked a
337 fixed indel in STE20-related kinase adapter protein alpha (STRAD α ; NCBI: LOC107340566,
338 Reef Genomics: *Acropora_digitifera_13579*) because it has a deletion of four-amino acids, along
339 with two amino acid substitutions in *A. palmata*, both of which are fixed differences between the
340 Caribbean Acroporids. It aligns well with human STRAD α , isoform 4 protein NP_001003788.1
341 (E-value 2e-77). A blastp search of coral resources indicates that the deletion is unique to *A.*
342 *palmata* (Figure S6B), although *Madracis auretenra* also has a four amino acid deletion, but
343 shifted by three positions. This deletion in *A. palmata* is confirmed by the lack of reads mapping
344 to the 12bp nucleotide region (Figure S7).

345 To determine the degree of protein modification from these differences, we positioned them
346 on a predicted protein structure of *A. cervicornis* using I-TASSER server (Yang et al. 2015).
347 Figure 3 illustrates the predicted configuration of the protein using as structural reference the
348 inactive STRAD α protein annotated by Zeqiraj et al. (2009). The indel occurring between *A.*
349 *palmata* and *A. cervicornis* is at positions 322 to 325, and the substitutions in positions 62 and
350 355. In order to induce the activation of STRAD α , ATP binds and induces a conformational
351 change. In its active stage, STRAD α interacts with MO25 α by means of the alpha-helices B, C
352 and E, the beta-laminae 4 and 5, and the activation loop to further regulate liver kinase B1
353 (LKB1) (Zeqiraj et al. 2009). Despite the fact that neither the substitutions nor the indel are
354 placed in the structural elements described to interact with ATP or MO25 α , it is difficult to
355 disregard their functional role with them or with LKB1.

356 **KEGG Pathways Enriched for Fixed SNVs**

357 An alternative to looking at individual amino acid substitutions is to search for protein
358 groupings that are enriched for substitutions. This is frequently done with Gene Ontology terms
359 (Consortium 2015) and/or classifications according to the KEGG (Kanehisa et al. 2017). We
360 took advantage of the *A. digitifera* KEGG pathway annotations and looked for KEGG classes
361 enriched for fixed amino acid variants. Five out of 119 pathways were found to be enriched in
362 non-synonymous substitutions between *A. palmata* and *A. cervicornis* (two-tailed Fisher's exact
363 test, $p < 0.05$), and included two pathways where up to 12 genes presented these differences (i.e.
364 ABC transporters and Wnt signaling pathway, Table 3). In Figure 4, the Wnt signaling pathway
365 and the 12 genes with a fixed difference out of 101 genes (approximately 12%) in this pathway
366 are displayed. Note that multiple genes in Table 3 can be mapped to the same module, and
367 several modules might appear more than once in Figure 4. In particular, these 12 genes added 27
368 non-synonymous fixed differences between *A. palmata* and *A. cervicornis*, and were grouped
369 into seven different modules within the pathway (i.e. Axin, beta-catecin, Frizzled, Notum,
370 SMAD4, SIP, and Wnt). Of these modules, Wnt grouped the largest number of genes ($n=5$),
371 followed by Frizzled ($n=2$), and all the other modules with just one gene. The Wnt module
372 included three WNT4 paralogue genes and nine non-synonymous mutations. Notably, the Axin
373 module included only one gene orthologue to AXIN1 (i.e. LOC107345943) but six non-
374 synonymous mutations. Similarly, the module Notum only includes one gene orthologue to
375 NOTUM but this gene has five non-synonymous fixed mutations between *A. palmata* and *A.*
376 *cervicornis*.

377 The strongest support from the KEGG analysis was for an enrichment of fixed amino acid
378 differences in 12 of 67 ABC transporters (Table 3). The 12 include orthologues of the following

379 three ATP-binding subfamily members: member 7 of subfamily B, member 2 of subfamily D
380 (ABCD2), and member 2 of subfamily G. Judged by the level of inter-species sequence
381 conservation around the variant position, ABCD2 stands out. ABCD2 transports fatty acids
382 and/or long chained fatty acyl-CoAs into the peroxisome (Andreoletti et al. 2017). The variant
383 valine (V) appears to at the beginning of transmembrane helices 3 that is conserved in the
384 majority of coral species, including *A. digitifera* and *A. cervicornis* (Figure S8). In *A. palmata*
385 and *A. millepora* the V is replaced by isoleucine (I). However, the residues predicted to stabilize
386 ABCD proteins and facilitate transport across the membrane are conserved between all corals
387 and the human orthologue (Andreoletti et al. 2017). In vertebrates, the “motif”
388 SVAHLYSNLTKPILDV is essentially conserved in all mammal, bird, and fish genomes
389 available at the UCSC browser (Figure S9). The only three substitutions pictured in Figure S9
390 are a somewhat distant I→V in hedgehog and rabbit, and V→I in opossum at the position variant
391 in *A. palmata*. This extreme level of inter-species protein conservation suggests that the ABCD2
392 orthologue may function somewhat differently in *A. palmata* and *A. millepora* compared to most
393 other corals. However, the ease with which V and I can be interchanged in nature, because of
394 their biochemical similarity and illustrated by the mammalian substitutions mentioned above,
395 tempers our confidence in this prediction. Still, the apparent near-complete conservation of this
396 particular valine in evolutionary history lends some weight to the hypothesis.

397 **Genomic Stretches of SNVs**

398 Rather than restricting the analyses to only the fixed SNVs, a larger set of the high-quality
399 SNVs related to the species differences can be identified by interrogating the joint allele-
400 frequency spectrum of the two species. An advantage of this approach over considering just

401 amino acid variants is that it can potentially detect functional changes in non-coding regions,
402 such as promoters or enhancers. We identified 12,279 intervals of consecutive SNVs with high
403 F_{ST} values. The genomic intervals ranged from 5 b (NW_015441140.1:321,729-321,734, 4
404 SNVs with average $F_{ST} = 1.0$) to 27 kb (NW_015441096.1: 814,882-842,464, 8 SNVs with
405 average $F_{ST} = 0.9217$). The top scoring interval covers a 14 kb window in positions 64,603-
406 78,897 of scaffold NW_015441181.1 (Table S5 and Figure 5A). The average F_{ST} for the 241
407 SNVs in this interval is 0.9821, while the average F_{ST} for all of the roughly 1.7 million SNVs is
408 0.1089. Within this interval, there are three gene models: methyltransferase-like protein 12
409 (MTL12; NCBI: LOC107339088), Wnt inhibitory factor 1-like protein (WIF1; NCBI:
410 LOC107339060), mucin-5AC-like protein (MUC5AC; NCBI: LOC107339062) (Figure 5A).

411 The next highest scoring run of high F_{ST} values is the 15 kb interval in positions 447289-
412 462570 of scaffold NW_015441116.1 (Figure 5B). The 306 SNVs in this region have an average
413 $F_{ST} = 0.9756$. The most recent NCBI gene annotations mention two intersecting genes in the
414 interval, protein disulfide-isomerase A5-like (PDIA5; NCBI: LOC107334364), mapping to the
415 interval 447,296-458,717, and thioredoxin domain-containing protein 12-like (TXNDC12;
416 NCBI: LOC107334366), mapping to 459,123-462,401 (Table S5 and Figure 5B). Adjacent to
417 this interval are three lower scoring intervals also containing a gene annotated as TXNDC12
418 (NCBI: LOC107334421), mapping to 463,276-467,160 (Table S5 and Figure 5B). The mapping
419 of LOC107334366 shows a strong match to seven exons, but the mapping of LOC107334364
420 include weakly aligning exons and missing splice signals. LOC107334364 consists of three
421 weakly conserved tandem repeats, and has partial blastn alignments to position 33-172 of human
422 thioredoxin domain-containing protein 12 precursor (GenBank: NP_056997.1). The shorter
423 sequence LOC107334366 has a blastp alignment (E-value $9e-22$) to the same region. In the older

424 Reef Genomics dataset for *A. digitifera*, the corresponding gene for LOC107334364 is
425 *Acropora_digitifera_140461*. Thus, based on the newer NCBI annotation, there appears to be
426 either a gene or a pseudo-gene in this highly divergent genomic region of *A. digitifera*.

427 **SNV Markers for Species Identification and Hybrid Assignment**

428 To aid the design of genotyping studies we identified 894 “PCR-ready” SNVs as those that
429 do not have another SNV, indel, or any (interspersed or tandemly duplicated) repeats within 50
430 bp (Table 2). We call these the “PCR-ready” SNVs, since in theory they are good candidates for
431 amplification in any of the three *Acropora* species. We validated a subset of eight of these PCR-
432 ready SNVs in additional *A. palmata* ($n=10$) and *A. cervicornis* ($n=9$) samples from across the
433 geographic range (Table S2) using a RFLP assay. The eight markers were designed to digest the
434 PCR product at a single nucleotide base present in only one of the two species (Table S3). For
435 example, at locus NW_015441435.1 position 299429, the variable base between the species (GG
436 in *A. cervicornis* and AA in *A. palmata*) provides a unique recognition site in *A. cervicornis* for
437 the restriction enzyme *HpyCH4IV* (A[^]CG_T) that results in digestion of *A. cervicornis* PCR
438 product but not *A. palmata* (Figure S11A). We found that our stringent selection of PCR-ready
439 SNVs are in fact fixed in the additional samples surveyed.

440 We also screened colonies that were morphologically classified as hybrids between *A.*
441 *palmata* and *A. cervicornis*. We attempted to refine the hybrid classification of colonies into first
442 or later generation hybrid groups based on the proportion of ancestry from each parental species
443 using five microsatellite markers or the above described eight SNV loci. .

444 Using the SNV makers, the reference F1 hybrids and seven later generation hybrids were
445 heterozygous at all variable sites, whereas the remaining later generation hybrids ($n=17$)

446 genotypes at each site varied depending on the locus (two examples in Figure S11). Similar to
447 the F1 hybrids, the test set of hybrids were also heterozygous at all loci. For each locus,
448 genotypes were scored to produce a multi-locus genotype (MLG) for each individual.

449 The congruency of taxon classification was compared between the SNV MLGs and
450 microsatellite MLGs using a discriminant factorial correspondence analysis (DFCA) for each
451 marker set (Figure 6). All *A. cervicornis* samples but one were correctly identified to their
452 taxonomic group using the microsatellite MLGs, but in only 50% of *A. palmata* colonies did the
453 microsatellite clustering coincide with the previous taxon assignment (Table S2 and Figure 6A).
454 In contrast, because of stringency in selecting the fixed SNV loci, there was 100% agreement of
455 the previous taxon assignment of the parental species colony and its SNV MLG classification
456 (thus data points for pure bred samples are overlaid by the group centroid in Figure 6B).

457 No hybrid samples (F1, later generation or those in the test set) were assigned with high
458 probability to the F1 group with either marker set in the DFCA (Table S2). However, we found
459 that the SNV MLGs of F1 hybrids, seven later generation hybrids and all test hybrids shared the
460 same discriminant function coordinates as the F1 centroid, representing F1-like hybrids in the
461 data set (overlaid by F1 group centroid in Figure 6B). The remaining later generation hybrids
462 were classified as either *A. cervicornis* ($n=6$), *A. palmata* ($n=1$) or hybrid ($n= 10$; Figure 6B and
463 Table S2).

464 **DISCUSSION**

465 In this study, we have identified inter- and intra-species SNVs and indels between three
466 *Acropora* species. These variants can cause amino acid substitutions that might ultimately alter
467 protein function between these corals. We provided examples of genes with putative fixed-

468 differences between the Caribbean Acroporid species, grouped variants by their KEGG
469 pathways, highlighting examples from the Wnt and ABC transporter pathways, identified highly
470 diverged genomic regions between them and developed a RFLP assay to distinguish species and
471 hybrids. Genomic resources and workflows are available on Galaxy allowing researchers to
472 reproduce the analyses in this paper and apply them to any Acroporid species or other non-model
473 organisms.

474 **Candidate Loci in Growth and Development**

475 Genes in the Wnt pathway are critical for pattern formation, tissue differentiation in
476 developing embryos and tissue regeneration of Cnidaria (Guder et al. 2006). Interestingly, we
477 found that genes in the Wnt pathway are enriched in fixed amino acid substitutions and an
478 antagonist of this pathway, WIF, has consecutive SNVs with high F_{ST} values between *A.*
479 *cervicornis* and *A. palmata*.

480 Wnt genes function in primary body axis determination in *Hydra* and *Nematostella*
481 (Hobmayer et al. 2000; Kusserow et al. 2005), and in bud and tentacle formation in *Hydra*
482 (Philipp et al. 2009). Changes in the expression of Wnt genes under high temperatures are
483 hypothesized to result in disassociating *A. palmata* embryos and planulae with bifurcated oral
484 pores, indicating the critical role of this pathway in the ability of coral larvae to develop properly
485 under thermal stress (Polato et al. 2013). The genomic differences in the Wnt genes between
486 elkhorn and staghorn corals reported here (Figure 4) could reflect developmental or growth
487 adaptations that may be influenced by temperature, underscoring the warning that changing
488 ocean temperature can alter the development of corals.

489 The Wnt pathway continues to regulate coral growth beyond early developmental life stages.
490 In the two Caribbean Acroporids, expression of Wnt genes was higher in the tips of colonies than
491 the base of colonies (Hemond et al. 2014). Differential expression of WIF was not observed in
492 the comparison of the distinct branch regions within or between species or under larval thermal
493 stress in *A. palmata* (Polato et al. 2013; Hemond et al. 2014), but WIF expression in *A. digitifera*
494 did change across the transitional life stages of blastula, gastrula, post-gastrula and planula
495 (Cruciat and Niehrs 2013; Reyes-Bermudez et al. 2016).

496 Another candidate gene STRAD α (Figure 3) is part of the AMP-activated protein kinase
497 (AMPK) pathway, which plays a key role in cellular growth, polarity and metabolism. Under
498 starvation or stressful conditions, the AMPK pathway senses cell energy and triggers a response
499 to inhibit cell proliferation and autophagy (Hawley et al. 2003). Recently, the switch towards
500 activation of AMPK-induced autophagy over apoptosis has been proposed to enhance disease
501 tolerance in immune stimulated corals (Fuess et al. 2017). In this study, STRAD α was found to
502 have two non-synonymous mutations and an indel between *A. cervicornis* and *A. palmata*
503 (Figure 3). Although these changes do not occur in a reported site of activity, we cannot ignore
504 the possibility that they are relevant in the interaction of STRAD α with MO25A α and LKB1.
505 The products of these three genes interact together to regulate the AMPK cascade, with
506 STRAD α being key for LKB1 protein stability. The extent to which AMPK more broadly
507 contributes to the development and disease tolerance of elkhorn and staghorn corals needs to be
508 further explored.

509 **Candidate Loci for Microbe Interactions and Cellular Stress**

510 We highlighted several genes with fixed differences between the two Caribbean Acroporids
511 that are involved in innate immunity, membrane transport and oxidative stress in cnidarians.
512 These genes are also important for mediating interactions between the coral host and their
513 microbial symbionts. Corals mediate interactions with foreign microbes by either creating
514 physical barriers or initiating an innate immune response (Palmer and Traylor-Knowles 2012;
515 Oren et al. 2013). Innate immunity is not only activated for the removal of threatening microbes,
516 but also facilitates colonization of beneficial microorganisms within the coral host.

517 As one of the physical barriers, corals secrete a viscous mucus on the surface of their
518 epithelium that can trap beneficial and pathogenic microbes (Sorokin 1973; Rohwer et al. 2002).
519 Microbial fauna of the mucus can form another line of defense for their host, with evidence that
520 mucus from healthy *A. palmata* inhibits growth of other invading microbes and contributes to the
521 coral antimicrobial activity (Ritchie 2006). This mucus is composed of mucins, one of which
522 might be mucin 5AC that was found to span three divergent genomic intervals between *A.*
523 *palmata* and *A. cervicornis*. Mucin-like proteins have been found in the skeletal organic matrix
524 of *A. millepora* (Ramos-Silva et al. 2014) and are differentially expressed in the tips of *A.*
525 *cervicornis* during the day (Hemond and Vollmer 2015) suggesting a potential role for these
526 large glycoproteins in biomineralization as well. Thus, the divergence of mucin in elkhorn and
527 staghorn corals could underlie difference in the composition of their mucus and/or calcification
528 patterns.

529 Beyond the mucus layer, corals and other cnidarians have a repertoire of innate immune
530 tools to recognize microbial partners from pathogens and remove the latter. The transcription
531 factor NF- κ B is one of these tools that regulates expression of immune effector genes, including

532 mucin mentioned above (Sikder et al. 2014). We identified two fixed SNVs in NKIRAS2, an
533 inhibitor of NF- κ B transcription (Chen et al. 2004). The two substitutions within this gene were
534 both unique to either *A. palmata* or *A. cervicornis* and neither were shared by the Pacific
535 Acroporids. While the role of NKIRAS1 and -2 are largely unexplored in non-mammal animals,
536 NKIRAS1 has been reported to be one out of nine genes down-regulated at high temperatures in
537 *A. palmata* (Polato et al. 2013).

538 As a way to interact and exchange nutrients with their beneficial microbes, corals can use
539 ABC transporter proteins. In general, ABC transporters encode for large membrane proteins that
540 can transport different compounds against a concentration gradient using ATP. More
541 specifically, they can transport long-chain fatty acids, enzymes, peptides, lipids, metals, mineral
542 and organic ions, and nitrate. ABC transporters were enriched in fixed amino acid differences
543 between *A. palmata* and *A. cervicornis* (Table 3). Previous characterization of the proteins
544 embedded in a sea anemone symbiosome, the compartment where the symbionts are housed,
545 found one ABC transporter which could facilitate movement of molecules between partners
546 (Peng et al. 2010). ABC transporters were upregulated in response to high CO₂ concentrations
547 (Kaniewska et al. 2012) and during the day (Bertucci et al. 2015) in *A. millepora* suggesting
548 diverse roles for these proteins, transporting both molecules from the environment and
549 metabolites from their symbionts.

550 Within the ABC transporters, we analyzed in detail the non-synonymous mutations in
551 ABCD2 between *A. palmata* and *A. cervicornis* (Figure S8). This analysis was limited by the
552 availability of sequences, but allowed us to conclude that the amino acid substitution, though
553 expected to not produce a large functional change, is embedded in a well conserved motif. The
554 ABCD2 product is involved in the transport of very long-chain acyl-CoA into peroxisomes for β -

555 oxidation. It has been reported that *A. palmata* larvae derive their energy by this mean and that
556 high temperatures induce a change in expression of genes associated with peroxisomal β -
557 oxidation (Polato et al. 2013). This is thought to indicate that larvae of *A. palmata* catabolize
558 their lipid stores more rapidly at elevated temperatures (Polato et al. 2013). Increased lipid
559 catabolism in turn drove the need for additional redox homeostasis proteins to deal with reactive
560 oxygen species (ROS) produced during oxidation of fatty acids (Polato et al. 2013).

561 Superoxide dismutase, PDIA5 and TXDNC12 are involved in ROS stress-response and
562 antioxidant defense to deal with the oxygen radicals that are produce via the coral host or its
563 symbionts. It has been reported that the antioxidant protein SOD, which converts superoxide
564 anions to hydrogen peroxide, is important to reduce the ROS produced by the coral host and also
565 its dinoflagellate symbiont (Levy et al. 2006), particularly under high temperature stress (Downs
566 et al. 2002), high photosynthetically active radiation (Downs et al. 2002) and salinity stress
567 (Gardner et al. 2016). The genes PDIA5 and TXDNC12 also regulate oxidative stress as well as
568 protein folding. They are both localized to the endoplasmic reticulum and belong to the
569 thioredoxin superfamily of proteins (Galligan and Petersen 2012). These genes were found to
570 span the longest interval of significant genomic differentiation between the two Caribbean
571 species (Figure 5). Thioredoxin-like genes have been differentially expressed in a number of
572 thermal stress experiments on Pacific Acroporids (Starcevic et al. 2010; Souter et al. 2011; Rosic
573 et al. 2014) providing strong support for their role in mediating redox stress. Future research is
574 required to validate the functional consequences of the substitutions in the loci that differ
575 between *A. palmata* and *A. cervicornis* and their putative roles in host cellular stress response,
576 microbial interactions and/or nutrient exchange.

577 **Mitochondrial SNVs**

578 Unlike other metazoan mitochondrial DNA (mtDNA), cnidarian mtDNA evolves much
579 slower and is almost invariant among conspecifics (van Oppen *et al.* 1999; Shearer *et al.* 2002).
580 However, the so-called control region can be hypervariable compared to the other mtDNA
581 regions in corals (Shearer *et al.* 2002), and is where the majority of the mitochondrial SNVs in
582 these taxa were identified (Figure S3). The variability in this gene-free region has been used in
583 previous studies to reconstruct the phylogenetic relationship all Acroporid species (van Oppen *et*
584 *al.* 2001) and as one of the markers to determine gene-flow between *A. palmata* and *A.*
585 *cervicornis* from hybridization (Vollmer & Palumbi 2002, 2007). The lack of fixed-differences
586 between the mtDNA of these two species suggests that mito-nuclear conflict might be limited or
587 non-existent during hybridization of these species.

588 **Species-Specific Diagnostic Markers**

589 We validated eight of the PCR-ready fixed SNVs in additional Acroporid samples and
590 classified the two Acroporid species and their hybrid based on the MLGs of these makers and
591 five microsatellite loci (Figure 6). Currently, microsatellite makers are routinely used to identify
592 Acroporid genotypes and clone mates, but only one of these is a species-specific marker (locus
593 192) between the Caribbean Acroporid (Baums *et al.* 2005; Baums *et al.* 2009). While previous
594 studies have used labor intensive Sanger-sequencing of one mitochondrial and three nuclear loci
595 to study Caribbean hybrid *Acropora* (Van Oppen *et al.* 2000; Vollmer and Palumbi 2002), PCR-
596 ready fixed SNV markers provide an alternative for high-throughput genotyping and hybrid
597 classification. The detection of only one variable base at each SNV locus can lower genotyping
598 error, avoid difficulties in interpreting heterozygous Sanger sequences and increase

599 reproducibility across labs (Anderson and Garza 2006). Our results indicate a small number of
600 fixed SNVs can outperform the microsatellite makers for taxonomic classification of the species
601 but not necessarily the hybrids. Our inability to discriminate the F1-like hybrids from the later
602 generation hybrids with the DFCA is likely due to the low sample size of reference F1 hybrids
603 ($n=3$). In the case of the SNV markers, the identical MLGs between the F1 hybrids and seven
604 later generation hybrids further reduced our ability to separate the groups. Therefore, with the
605 limited number of PCR-ready SNVs tested, there was no difference in the performance of
606 microsatellite to SNV loci for refining hybrid classification. These results however, indicate that
607 the genomes provide a rich source for PCR-ready SNVs albeit a larger number of SNVs than
608 tested here will need to be assayed before Caribbean Acroporid hybrids can be classified
609 confidently.

610 **CONCLUSION**

611 By using the genome assembly of *A. digitifera*, we were able to detect differences between
612 *A. cervicornis* and *A. palmata* at various levels, from a single nucleotide substitution to hundreds
613 of nucleotide substitutions over large genomic intervals. We identified genetic differences in key
614 pathways and genes known to be important in the animals' response to the environmental
615 disturbances and larval development. This project can work as a pilot to gather intra- and
616 interspecies differences between *A. cervicornis* and *A. palmata* across their geographic range.
617 Ultimately, gene knock-down and gene editing experiments are needed to test whether these and
618 other genetic differences have functional consequences and thus could be targets for improving
619 temperature tolerance and growth of corals.

620 **WEB RESOURCES**

621 The SNV and indel calls for both the nuclear and mitochondrial genomes are available at the
622 Galaxy internet server (usegalaxy.org) (Afgan et al. 2016).

623 **DATA AVAILABILITY**

624 NCBI Accession numbers for the raw reads are SRR7235977-SRR7236038. Supplemental
625 figures and tables are uploaded to figshare (link).

626 **ACKNOWLEDGMENTS**

627 This study was funded by NSF OCE-1537959 to IBB, NF, and WM. Thanks to the PSU
628 genomics facility for performing the sequencing. Additional thanks to Meghann Devlin-Durante
629 for assistance with DNA extractions and Macklin Elder for help with the RFLP assay. Samples
630 were collected and exported with appropriate permits.

631 **AUTHOR CONTRIBUTIONS**

632 AR provided SNV and indel calls and produced the figure of mitochondrial variants. SK
633 extracted the coral DNA, contributed to the analysis of the SNVs and developed and analyzed
634 the RFLP assay. OB generated 3D protein model and performed KEGG pathway enrichment
635 analysis. RB made the variants available on Galaxy. NF provided samples for the genome
636 sequencing and RFLP validation. AR, SK, OB, WM and IBB wrote the paper. The project is
637 being managed by IBB.

638

639 **LITERATURE CITED**

- 640 Afgan, E., D. Baker, M. Van den Beek, D. Blankenberg, D. Bouvier *et al.*, 2016 The Galaxy
641 platform for accessible, reproducible and collaborative biomedical analyses: 2016 update.
642 *Nucleic Acids Research* 44 (W1):W3-W10.
- 643 Agaba, M., E. Ishengoma, W.C. Miller, B.C. McGrath, C.N. Hudson *et al.*, 2016 Giraffe genome
644 sequence reveals clues to its unique morphology and physiology. *Nature*
645 *Communications* 7:11519.
- 646 Akey, J.M., G. Zhang, K. Zhang, L. Jin, and M.D. Shriver, 2002 Interrogating a high-density
647 SNP map for signatures of natural selection. *Genome Research* 12 (12):1805-1814.
- 648 Altschul, S.F., T.L. Madden, A.A. Schäffer, J. Zhang, Z. Zhang *et al.*, 1997 Gapped BLAST and
649 PSI-BLAST: a new generation of protein database search programs. *Nucleic Acids*
650 *Research* 25 (17):3389-3402.
- 651 Anderson, E., and E. Thompson, 2002 A model-based method for identifying species hybrids
652 using multilocus genetic data. *Genetics* 160 (3):1217-1229.
- 653 Anderson, E.C., and J.C. Garza, 2006 The power of single-nucleotide polymorphisms for large-
654 scale parentage inference. *Genetics* 172 (4):2567-2582.
- 655 Andreoletti, P., Q. Raas, C. Gondcaille, M. Cherkaoui-Malki, D. Trompier *et al.*, 2017 Predictive
656 structure and topology of peroxisomal ATP-binding cassette (ABC) transporters.
657 *International Journal of Molecular Sciences* 18 (7):1593.
- 658 Anonymous, 2006 Endangered and threatened species: final listing determinations for elkhorn
659 coral and staghorn coral. *Federal Register* 71:26852-26872.

- 660 Baums, I., M. Devlin - Durante, L. Brown, and J. Pinzón, 2009 Nine novel, polymorphic
661 microsatellite markers for the study of threatened Caribbean acroporid corals. *Molecular*
662 *Ecology Resources* 9 (4):1155-1158.
- 663 Baums, I.B., 2008 A restoration genetics guide for coral reef conservation. *Molecular Ecology*
664 17 (12):2796-2811.
- 665 Baums, I.B., C.R. Hughes, and M.E. Hellberg, 2005 Mendelian microsatellite loci for the
666 Caribbean coral *Acropora palmata*. *Marine Ecology Progress Series* 288:115-127.
- 667 Bedoya-Reina, O.C., A. Ratan, R. Burhans, H.L. Kim, B. Giardine *et al.*, 2013 Galaxy tools to
668 study genome diversity. *Gigascience* 2 (1):17.
- 669 Belkhir, K., P. Borsa, L. Chikhi, N. Raufaste, and F. Bonhomme, 2004 GENETIX 4.05,
670 Windows TM software for population genetics. *Laboratoire génome, populations,*
671 *interactions, CNRS UMR 5000*.
- 672 Bertucci, A., S. Foret, E. Ball, and D.J. Miller, 2015 Transcriptomic differences between day and
673 night in *Acropora millepora* provide new insights into metabolite exchange and light -
674 enhanced calcification in corals. *Molecular Ecology* 24 (17):4489-4504.
- 675 Bhattacharya, D., S. Agrawal, M. Aranda, S. Baumgarten, M. Belcaid *et al.*, 2016 Comparative
676 genomics explains the evolutionary success of reef-forming corals. *eLife* 5:e13288.
- 677 Bruckner, A.W., 2002 *Acropora* Workshop: Potential Application of the US Endangered Species
678 Act as a Conservation Strategy. *NOAA Technical Memorandum NMFS-OPR*.
- 679 Cairns, S.D., 1982 Stony corals (Cnidaria: Hydrozoa, Scleractinia) of Carrie Bow Cay, Belize.
- 680 Chang, H.-W., Y.-H. Cheng, L.-Y. Chuang, and C.-H. Yang, 2010 SNP-RFLPing 2: an updated
681 and integrated PCR-RFLP tool for SNP genotyping. *BMC Bioinformatics* 11 (1):173.

- 682 Chang, H.-W., C.-H. Yang, P.-L. Chang, Y.-H. Cheng, and L.-Y. Chuang, 2006 SNP-RFLPing:
683 restriction enzyme mining for SNPs in genomes. *BMC Genomics* 7 (1):30.
- 684 Chen, Y., S. Vallee, J. Wu, D. Vu, J. Sondek *et al.*, 2004 Inhibition of NF- κ B activity by I κ B β in
685 association with κ B-Ras. *Molecular and Cellular Biology* 24 (7):3048-3056.
- 686 Consortium, G.O., 2015 Gene ontology consortium: going forward. *Nucleic Acids Research* 43
687 (D1):D1049-D1056.
- 688 Cruciat, C.-M., and C. Niehrs, 2013 Secreted and transmembrane wnt inhibitors and activators.
689 *Cold Spring Harbor Perspectives in Biology* 5 (3):a015081.
- 690 Downs, C., J.E. Fauth, J.C. Halas, P. Dustan, J. Bemiss *et al.*, 2002 Oxidative stress and seasonal
691 coral bleaching. *Free Radical Biology and Medicine* 33 (4):533-543.
- 692 Drury, C., K.E. Dale, J.M. Panlilio, S.V. Miller, D. Lirman *et al.*, 2016 Genomic variation
693 among populations of threatened coral: *Acropora cervicornis*. *BMC Genomics* 17
694 (1):286.
- 695 Faust, G.G., and I.M. Hall, 2014 SAMBLASTER: fast duplicate marking and structural variant
696 read extraction. *Bioinformatics* 30 (17):2503-2505.
- 697 Fuess, L.E., E. Weil, R.D. Grinshpon, and L.D. Mydlarz, 2017 Life or death: disease-tolerant
698 coral species activate autophagy following immune challenge. *Proceedings of the Royal*
699 *Society of London, Series B: Biological Sciences* 284 (1856):20170771.
- 700 Galligan, J.J., and D.R. Petersen, 2012 The human protein disulfide isomerase gene family.
701 *Human genomics* 6 (1):6.
- 702 Gardner, S.G., D.A. Nielsen, O. Laczka, R. Shimmon, V.H. Beltran *et al.*, 2016
703 Dimethylsulfoniopropionate, superoxide dismutase and glutathione as stress response

- 704 indicators in three corals under short-term hyposalinity stress. *Proc. R. Soc. B* 283
705 (1824):20152418.
- 706 Guder, C., I. Philipp, T. Lengfeld, H. Watanabe, B. Hobmayer *et al.*, 2006 The Wnt code:
707 cnidarians signal the way. *Oncogene* 25 (57):7450-7460.
- 708 Hawley, S.A., J. Boudeau, J.L. Reid, K.J. Mustard, L. Udd *et al.*, 2003 Complexes between the
709 LKB1 tumor suppressor, STRAD α/β and MO25 α/β are upstream kinases in the AMP-
710 activated protein kinase cascade. *Journal of Biology* 2 (4):28.
- 711 Hemond, E.M., S.T. Kaluziak, and S.V. Vollmer, 2014 The genetics of colony form and function
712 in Caribbean *Acropora* corals. *BMC Genomics* 15 (1):1133.
- 713 Hemond, E.M., and S.V. Vollmer, 2015 Diurnal and nocturnal transcriptomic variation in the
714 Caribbean staghorn coral, *Acropora cervicornis*. *Molecular Ecology* 24 (17):4460-4473.
- 715 Hobmayer, B., F. Rentzsch, K. Kuhn, C.M. Happel, C.C. von Laue *et al.*, 2000 WNT signalling
716 molecules act in axis formation in the diploblastic metazoan *Hydra*. *Nature* 407:186.
- 717 Holsinger, K.E., and B.S. Weir, 2009 Genetics in geographically structured populations:
718 defining, estimating and interpreting FST. *Nature Reviews Genetics* 10 (9):639-650.
- 719 Howe, K., A. Bateman, and R. Durbin, 2002 QuickTree: building huge Neighbour-Joining trees
720 of protein sequences. *Bioinformatics* 18 (11):1546-1547.
- 721 Hubisz, M.J., K.S. Pollard, and A. Siepel, 2010 PHAST and RPHAST: phylogenetic analysis
722 with space/time models. *Briefings in bioinformatics* 12 (1):41-51.
- 723 Kanehisa, M., M. Furumichi, M. Tanabe, Y. Sato, and K. Morishima, 2017 KEGG: new
724 perspectives on genomes, pathways, diseases and drugs. *Nucleic Acids Research* 45
725 (D1):D353-D361.

- 726 Kaniewska, P., P.R. Campbell, D.I. Kline, M. Rodriguez-Lanetty, D.J. Miller *et al.*, 2012 Major
727 Cellular and Physiological Impacts of Ocean Acidification on a Reef Building Coral.
728 *PLoS ONE* 7 (4):e34659.
- 729 Kent, W.J., C.W. Sugnet, T.S. Furey, K.M. Roskin, T.H. Pringle *et al.*, 2002 The human genome
730 browser at UCSC. *Genome Research* 12 (6):996-1006.
- 731 Kusserow, A., K. Pang, C. Sturm, M. Hroudá, J. Lentfer *et al.*, 2005 Unexpected complexity of
732 the Wnt gene family in a sea anemone. *Nature* 433 (7022):156.
- 733 Levy, O., Y. Achituv, Y. Yacobi, N. Stambler, and Z. Dubinsky, 2006 The impact of spectral
734 composition and light periodicity on the activity of two antioxidant enzymes (SOD and
735 CAT) in the coral *Favia fava*. *Journal of Experimental Marine Biology and Ecology* 328
736 (1):35-46.
- 737 Li, H., 2011 A statistical framework for SNP calling, mutation discovery, association mapping
738 and population genetical parameter estimation from sequencing data. *Bioinformatics* 27
739 (21):2987-2993.
- 740 Li, H., and R. Durbin, 2009 Fast and accurate short read alignment with Burrows–Wheeler
741 transform. *Bioinformatics* 25 (14):1754-1760.
- 742 Li, H., B. Handsaker, A. Wysoker, T. Fennell, J. Ruan *et al.*, 2009 The sequence alignment/map
743 format and SAMtools. *Bioinformatics* 25 (16):2078-2079.
- 744 Liew, Y.J., M. Aranda, and C.R. Voolstra, 2016 Reefgenomics. Org-a repository for marine
745 genomics data. *Database* 2016.
- 746 Nekrutenko, A., and J. Taylor, 2012 Next-generation sequencing data interpretation: enhancing
747 reproducibility and accessibility. *Nature Reviews Genetics* 13 (9):667.

- 748 Novembre, J., T. Johnson, K. Bryc, Z. Kutalik, A.R. Boyko *et al.*, 2008 Genes mirror geography
749 within Europe. *Nature* 456 (7218):98-101.
- 750 Oren, M., G. Paz, J. Douek, A. Rosner, K.O. Amar *et al.*, 2013 Marine invertebrates cross phyla
751 comparisons reveal highly conserved immune machinery. *Immunobiology* 218 (4):484-
752 495.
- 753 Palmer, C.V., and N. Traylor-Knowles, 2012 Towards an integrated network of coral immune
754 mechanisms. *Proceedings of the Royal Society of London, Series B: Biological Sciences*
755 279 (1745):4106-4114.
- 756 Peng, S.E., Y.B. Wang, L.H. Wang, W.N.U. Chen, C.Y. Lu *et al.*, 2010 Proteomic analysis of
757 symbiosome membranes in Cnidaria–dinoflagellate endosymbiosis. *Proteomics* 10
758 (5):1002-1016.
- 759 Philipp, I., R. Aufschnaiter, S. Özbek, S. Pontasch, M. Jenewein *et al.*, 2009 Wnt/ β -catenin and
760 noncanonical Wnt signaling interact in tissue evagination in the simple eumetazoan
761 *Hydra*. *Proceedings of the National Academy of Sciences* 106 (11):4290-4295.
- 762 Polato, N.R., N.S. Altman, and I.B. Baums, 2013 Variation in the transcriptional response of
763 threatened coral larvae to elevated temperatures. *Molecular Ecology* 22 (5):1366-1382.
- 764 Ramos-Silva, P., J. Kaandorp, F. Herbst, L. Plasseraud, G. Alcaraz *et al.*, 2014 The skeleton of
765 the staghorn coral *Acropora millepora*: molecular and structural characterization. *PLoS*
766 *One* 9 (6):e97454.
- 767 RCoreTeam, 2017 R: A language and environment for statistical computing [Online]. R
768 Foundation for Statistical Computing, Vienna, Austria.
- 769 Reich, D., K. Thangaraj, N. Patterson, A.L. Price, and L. Singh, 2009 Reconstructing Indian
770 population history. *Nature* 461 (7263):489-494.

- 771 Reyes-Bermudez, A., A. Villar-Briones, C. Ramirez-Portilla, M. Hidaka, and A.S. Mikheyev,
772 2016 Developmental progression in the coral *Acropora digitifera* is controlled by
773 differential expression of distinct regulatory gene networks. *Genome Biology and*
774 *Evolution* 8 (3):851-870.
- 775 Richards, Z., D. Miller, and C. Wallace, 2013 Molecular phylogenetics of geographically
776 restricted *Acropora* species: Implications for threatened species conservation. *Molecular*
777 *Phylogenetics and Evolution* 69 (3):837-851.
- 778 Ritchie, K.B., 2006 Regulation of microbial populations by coral surface mucus and mucus-
779 associated bacteria. *Marine Ecology Progress Series* 322:1-14.
- 780 Rohwer, F., V. Seguritan, F. Azam, and N. Knowlton, 2002 Diversity and distribution of coral-
781 associated bacteria. *Marine Ecology Progress Series* 243:1-10.
- 782 Rosic, N., P. Kaniewska, C.-K.K. Chan, E.Y.S. Ling, D. Edwards *et al.*, 2014 Early
783 transcriptional changes in the reef-building coral *Acropora aspera* in response to thermal
784 and nutrient stress. *BMC Genomics* 15 (1):1052.
- 785 Shearer, T.L., M.J.H. Van Oppen, S.L. Romano, and G. Worheide, 2002 Slow mitochondrial
786 DNA sequence evolution in the Anthozoa (Cnidaria). *Molecular Ecology* 11 (12):2475-
787 2487.
- 788 Shinzato, C., E. Shoguchi, T. Kawashima, M. Hamada, K. Hisata *et al.*, 2011 Using the
789 *Acropora digitifera* genome to understand coral responses to environmental change.
790 *Nature* 476 (7360):320-323.

- 791 Sikder, M., H.J. Lee, M. Mia, S.H. Park, J. Ryu *et al.*, 2014 Inhibition of TNF - α - induced
792 MUC5AC mucin gene expression and production by wogonin through the inactivation of
793 NF - κ B signaling in airway epithelial cells. *Phytotherapy Research* 28 (1):62-68.
- 794 Sorokin, Y.I., 1973 Trophical role of bacteria in the ecosystem of the coral reef. *Nature* 242
795 (5397):415.
- 796 Souter, P., L. Bay, N. Andreakis, N. Csaszar, F. Seneca *et al.*, 2011 A multilocus, temperature
797 stress - related gene expression profile assay in *Acropora millepora*, a dominant reef -
798 building coral. *Molecular Ecology Resources* 11 (2):328-334.
- 799 Starcevic, A., W.C. Dunlap, J. Cullum, J.M. Shick, D. Hranueli *et al.*, 2010 Gene expression in
800 the scleractinian *Acropora microphthalma* exposed to high solar irradiance reveals
801 elements of photoprotection and coral bleaching. *PloS One* 5 (11):e13975.
- 802 Untergasser, A., I. Cutcutache, T. Koressaar, J. Ye, B.C. Faircloth *et al.*, 2012 Primer3—new
803 capabilities and interfaces. *Nucleic Acids Research* 40 (15):e115.
- 804 Van Oppen, M., B. Willis, H. Van Vugt, and D. Miller, 2000 Examination of species boundaries
805 in the *Acropora cervicornis* group (Scleractinia, Cnidaria) using nuclear DNA sequence
806 analyses. *Molecular Ecology* 9 (9):1363-1373.
- 807 van Oppen, M.J., J.K. Oliver, H.M. Putnam, and R.D. Gates, 2015 Building coral reef resilience
808 through assisted evolution. *Proceedings of the National Academy of Sciences* 112
809 (8):2307-2313.
- 810 van Oppen, M.J.H., B.J. McDonald, B. Willis, and D.J. Miller, 2001 The evolutionary history of
811 the coral genus *Acropora* (Scleractinia, Cnidaria) based on a mitochondrial and a nuclear

812 marker: Reticulation, incomplete lineage sorting, or morphological convergence?
813 *Molecular Biology and Evolution* 18 (7):1315-1329.

814 Vollmer, S.V., and S.R. Palumbi, 2002 Hybridization and the evolution of reef coral diversity.
815 *Science* 296 (5575):2023-2025.

816 Yang, J., R. Yan, A. Roy, D. Xu, J. Poisson *et al.*, 2015 The I-TASSER Suite: protein structure
817 and function prediction. *Nature Methods* 12 (1):7-8.

818 Zeqiraj, E., B.M. Filippi, S. Goldie, I. Navratilova, J. Boudeau *et al.*, 2009 ATP and MO25 α
819 regulate the conformational state of the STRAD α pseudokinase and activation of the
820 LKB1 tumour suppressor. *PLoS Biology* 7 (6):e1000126.

821

822 **TABLES**

823 **Table 1. Sequenced Genomes. Species assignment was based initially on microsatellite**

824 **multilocus genotyping.** *Acropora* Genet ID is an identifier for each *Acropora* multilocus

825 microsatellite genotype in the Baums Lab database. Coordinates are given in decimal degrees

826 (WGS84). Two samples were sequenced to a greater depth (bold type).

827

Species	Region	Sample ID	<i>Acropora</i> Genet ID	Reef	Latitude	Longitude	Collection Date	SRA Accession
<i>A. cervicornis</i>	Belize	CBE13827	C1630	Glovers Atoll	16.88806	-87.75973	8-Nov-15	SRR7236033
		CBE13837	C1631	Glovers Atoll	16.88806	-87.75973	8-Nov-15	SRR7236028
		CBE13792	C1632	Sandbores	16.77913	-88.11755	7-Nov-15	SRR7236031
		CBE13797	C1646	Sandbores	16.77913	-88.11755	7-Nov-15	SRR7236034
		CBE13786	C1569	South Carrie Bow Cay	16.80132	-88.0825	6-Nov-15	SRR7236032
	Curacao	CCU13917	C1648	Directors Bay	12.066	-68.85997	4-Feb-16	SRR7236036
		CCU13925	C1649	East Point	12.04069	-68.78301	5-Feb-16	SRR7235996
		CCU13901	C1647	SeaAquarium	12.0842	-68.8966	2-Feb-16	SRR7236030
		CCU13903	C1650	SeaAquarium	12.0842	-68.8966	2-Feb-16	SRR7236029
		CCU13905	C1651	SeaAquarium	12.0842	-68.8966	2-Feb-16	SRR7236037
	Florida	CFL4927	C1471	CRF	25.2155	-80.60778	22-Nov-11	SRR7235993
		CFL4959	C1476	CRF	24.9225	-81.12417	22-Nov-11	SRR7235991
		CFL4923	C1484	CRF	25.16472	-80.59389	22-Nov-11	SRR7235994
		CFL4928	C1485	CRF	25.03222	-80.50417	22-Nov-11	SRR7235992
		CFL14120	C1297	CRF (Grassy Key)	24.71182	-80.94595	1-Mar-16	SRR7235995
	USVI	CFL4960	C1297	CRF (Grassy Key)	24.71182	-80.94595	22-Nov-11	SRR7235990
		CVI13712	C1633	Botany	18.3569	-65.03515	28-Oct-15	SRR7235999
		CVI13696	C1638	Botany	18.3569	-65.03515	27-Oct-15	SRR7235989
		CVI13758	C1456	Flat Key	18.31701	-64.9892	31-Oct-15	SRR7236022
		CVI13714	C1644	Hans Lollik	18.40191	-64.9063	29-Oct-15	SRR7235998
<i>A. palmata</i>	Belize	CVI13738	C1628	Sapphire	18.3333	-64.8499	30-Oct-15	SRR7236021
		PBE13813	P2947	Glovers Atoll	16.88806	-87.75973	8-Nov-15	SRR7236017
		PBE13819	P2959	Glovers Atoll	16.88806	-87.75973	8-Nov-15	SRR7236015
		PBE13801	P2964	Sandbores	16.77913	-88.11755	7-Nov-15	SRR7236020
		PBE13784	P2945	South Carrie Bow Cay	16.80132	-88.0825	5-Nov-15	SRR7236019
	Curacao	PBE13815	P2951	South Carrie Bow Cay	16.80132	-88.0825	5-Nov-15	SRR7236018
		PCU13919	P2970	Directors Bay	12.066	-68.85998	4-Feb-16	SRR7235988
		PCU13933	P2977	East Point	12.04069	-68.78301	5-Feb-16	SRR7235987
		PCU13911	P1232	SeaAquarium	12.0842	-68.8966	3-Feb-16	SRR7235985
		PCU13907	P2212	SeaAquarium	12.0842	-68.8966	3-Feb-16	SRR7235986
	Florida	PCU13939	P2976	Water Factory	12.1085	-68.9528	6-Feb-16	SRR7235982
		PFL5524	P2118	Carysfort	25.22178	-80.2106	1-Aug-05	SRR7236012
		PFL2655	P1032	Elbow	25.14363	-80.25793	3-Jun-10	SRR7235979
		PFL2699	P2564	French	25.03393	-80.34941	28-May-10	SRR7236011
		PFL1012	P1000	Horseshoe	25.13947	-80.29435	25-Apr-01	SRR7235983
	USVI	PFL1037	P1001	Little Grecian	25.11843	-80.31715	2-Jul-02	SRR7235980
		PFL6895	P1003	Sand Island	25.01817	-80.36832	17-Sep-09	SRR7236001
		PVI13702	P2957	Botany	18.3569	-65.03515	27-Oct-15	SRR7236003
		PVI13752	P2946	Flat Key	18.31701	-64.9892	31-Oct-15	SRR7236010
		PVI13744	P2953	Hans Lollik	18.40191	-64.9063	29-Oct-15	SRR7236008
USVI	PVI13750	P2954	Hans Lollik	18.40191	-64.9063	29-Oct-15	SRR7236009	
	PVI13740	P2952	Sapphire	18.3333	-64.8499	30-Oct-15	SRR7236007	

828 **Table 2. Data sets available on Galaxy.**

829

Name	Contents	# of Lines
SNVs	<i>A. digitifera</i> scaffold positions with two observed nucleotides among the three <i>Acropora</i> genomes	8,368,985
indels	positions and contents of observed short (≤ 20 bp) insertion/deletions	940,345
SAPs	protein sequence positions of non-synonymous and synonymous substitutions	561,015
mitochondrial SNVs	<i>A. digitifera</i> mitochondrial genome positions with two observed nucleotides	172
mitochondrial indels	position of an insertion/deletion	1
exons	scaffold positions of annotated exon endpoints	222,156
PCR-ready SNVs	SNVs where no other SNV, indel, or low-complexity sequence is within 50 bp	894

830

831 **Table 3. Statistically significant KEGG pathways enriched for genes having a fixed amino**

832 **acid difference between *A. cervicornis* and *A. palmata*.** The third column gives the number of

833 genes in the pathway with one or more fixed difference(s), and the third reports what fraction

834 they represent of all genes in the pathway. For instance, 67 of the genes are annotated as

835 belonging to the ABC transporter pathway, and $12/67 = 0.18$. Statistical significance determined

836 using a two-tailed Fisher's exact test.

837

Pathway	p-value	# Genes	Fraction
adf02010=ABC transporters	0.0015	12	0.18
adf00790=Folate biosynthesis	0.019	5	0.21
adf03420=Nucleotide excision repair	0.031	7	0.15
adf04933=AGE-RAGE signaling pathway in diabetic complications	0.023	9	0.14
adf04310=Wnt signaling pathway	0.037	12	0.12

838 **FIGURES**

839 **Figure 1. Phylogeny of corals with genomic and transcriptomic resources used in this study**

840 **(A) with images of the two focal species, *Acropora palmata* (B) and *Acropora cervicornis* (C).**

841 The evolutionary relationships depicted in the coral phylogeny are redrawn based on the

842 phylogenomic analysis by Bhattacharya *et al.* (2016), but branch lengths do not reflect

843 evolutionary distance. Estimate of divergence time between the Caribbean Acroporids and *A.*

844 *digitifera* was calculated by Richards *et al.* (2013). Photographs of *A. palmata* (B) and *A.*

845 *cervicornis* (C) were taken by Iliana B. Baums (Curacao 2018).

846

847 **Figure 2. Geographic origin of *Acropora* samples (A) and Principal Components Analysis**

848 **of *A. cervicornis* samples, five from each of four locations (B).** As noted in analyses of other

849 datasets (e.g., Novembre *et al.* (2008)) the geographic map is similar to the PCA.

850

851 **Figure 3. Predicted structure for STRAD α in *A. cervicornis*.** In its inactive conformation,

852 ATP binds the protein to activate it (in the space delimited by the purple residues). After the

853 protein is active, STRAD α interacts with MO25 to regulate LKB1. This interaction occurs by

854 means of the alpha-helices B, C and E, the beta-laminae 4 and 5, and the activation loop (blue).

855 *A. palmata* differs from *A. cervicornis* in two amino acids (N62Y and P355S) as well as in four

856 insertions (R322, D323, G324 and G325).

857

858 **Figure 4. Pictorial representation of the KEGG pathway for WNT signaling.** The red shaded
859 boxes indicate the genes having fixed amino acid differences between *A. cervicornis* and *A.*
860 *palmata*. Green indicates the genes that were found in these genomes but did not differ between
861 the species. White indicates the genes that were not found in the three Acroporid genomes.

862

863 **Figure 5. Genomic intervals with or without regions of differentiation between *A. palmata***
864 **and *A. cervicornis*.** Inter-species allelic differentiation (F_{ST}) was calculated using the unbiased
865 Reich-Patterson estimator (Reich et al. 2009). Intervals of high scoring SNVs were identified by
866 subtracting 0.90 from each SNV F_{ST} value and totaling the score of consecutive SNVs until the
867 score could no longer be increased by an additional SNV on either end. High scoring regions are
868 shaded in light grey along 60 kb genomic windows for the top two scoring intervals, scaffold
869 NW_015441181.1 (A) and scaffold NW_015441116.1 (B), compared to 60 kb genomic window
870 on scaffold NW_015441064.1 with no intervals (C). Grey points are the F_{ST} estimate for each
871 SNVs and blue line is the average F_{ST} calculated over 1 kb sliding window analysis. Predicted
872 genes within these windows are shown above the graph in grey arrows. In order, genes include
873 mitochondrial proton/calcium exchanger protein (LETM1), *A. digitifera* LOC107339089,
874 protein-L-isoaspartate(D-aspartate) O-methyltransferase (PCMT1), mitochondrial
875 methyltransferase-like protein 12 (MTL12), Wnt inhibitory factor 1 (WIF1), mucin-5AC-like
876 (MUC5AC), G protein-coupled receptor 9 (GPCR9), Ras-related and estrogen-regulated growth
877 inhibitor (RERG), protein disulfide-isomerase A5 (PDIA5), thioredoxin domain containing
878 protein (TXNDC), protein ABHD14B (ABHD14B), mitogen-activated protein kinase kinase

879 kinase kinase 4 (MAP4K4), poly(ADP-ribose) polymerase family member 15 (PARP15), *A.*
880 *digitifera* LOC107341429, and *A. digitifera* LOC107341151.

881 **Figure 6. Discriminant factorial correspondence analysis of five microsatellite markers (A)**
882 **and eight species-specific SNV loci (B).** Samples were assigned to four different groups based
883 on their previous taxon assignment: 1. *A. cervicornis* ($n=9$, blue upside down triangles), 2. *A.*
884 *palmata* ($n=10$, pink triangles), 3. F1 hybrids ($n=3$, purple squares), and 4. later generation
885 hybrids ($n=24$, green diamonds). The remaining hybrid samples ($n=20$, yellow circles) had no
886 previous hybrid assignment and acted as our test set for the analysis. The large shapes for each
887 group represent the group centroid, or mean. In panel B, data points for pure bred colonies are
888 not visible because their coordinates are identical to their respective group centroids. F1 hybrids,
889 test hybrids and seven later generation hybrids are also masked as they share the same
890 coordinates as the F1 centroid, representing F1-like hybrids in the data set.

891 **SUPPLEMENTAL DATA**

892 **Table S1. Alignment summary statistics for the various samples included in this study.**

893 **Each row corresponds to a sample.** The column ‘Generated Reads’ refers to the number of
894 sequences generated for the sample. ‘Mapped Reads’ refers to the sequences that aligned with a
895 mapping quality > 0, and ‘Properly Paired’ refers to the number of reads that align within the
896 expected distance from their mate. ‘Duplicate Reads’ refers to the number of reads that were
897 flagged as putative PCR duplicates. ‘Aligned Reads’ refers to the number of sequences that were
898 aligned to the *A. digitifera* reference using BWA, We present these statistics at both the sequence
899 and the base level. Samples 1012 and 14120 are the deeply sequenced samples.

900

901 **Table S2. Results from the discriminant factorial correspondence analysis for the**
902 **microsatellite and fixed SNV markers.** . Bold clonal IDs indicate repetitive genotypes and grey
903 rows highlight samples where the probability of membership from the discriminant factorial
904 correspondence analysis differs between the two marker sets. For example, sample 2984 was
905 identified as *A. cervicornis* based on morphology and previous posterior probabilities from a
906 NEWHYBRIDS analysis. The discriminant analysis assigned the sample 2984 with 71.53%
907 probability to the hybrid group using the Msat MLG. This is in contrast to the SNP MLG which
908 classified the sample with 96.7 % as being *A. cervicornis* in agreement with both the visual
909 identification and NEWHYBRIDS results.

910

911 **Table S3. Summary of the eight fixed SNV markers used to assign hybrids and species.** For
912 each SNV, the left nucleotide matches *A. cervicornis* and the right nucleotide matches *A.*
913 *palmata*.

914

915 **Table S4. Fixed SNV marker gene annotation.**

916 **Table S5. Gene models identified in the two highest scoring F_{ST} intervals between the 20**
917 **samples of *A. cervicornis* and *A. palmata*.**

918

919 **Figure S1. Genome coverage distributions of the 21 *Acropora cervicornis* samples.**

920

921 **Figure S2. Distance-based phylogenetic tree of the 42 newly sequenced *Acropora* samples.**

922

923 **Figure S3. Locations of 172 SNVs and one indel identified in the mitochondrial genome.**

924

925 **Figure S4. Superoxide dismutase alignment highlighting the SNV between *A. cervicornis***
926 **and *A. digitifera* (Reef Genomics:12779).**

927

928 **Figure S5. Alignment of NF-kappa-B inhibitor-interacting Ras-like protein 1 from**
929 ***Acropora digitifera*_6635 to sequences from other corals and the human orthologue**
930 **(GenBank: NP_065078.1).**

931

932 **Figure S6. STE20-related kinase adapter protein alpha isoform 4 (STRAD α) truncated**
933 **alignment of *A. digitifera* protein Reef Genomics: *Acropora_digitifera_13579*) with coral**
934 **sequences and human NP_001003788.1 to highlight fixed SNVs and indel in *A. palmata*.**

935

936 **Figure S7. Image of the coverage by sequenced reads around the 12-bp deletion of**
937 **STRAD α , showing unanimous agreement of the species difference, for *A. palmata* (A) and *A.***
938 ***cervicornis* (B).**

939

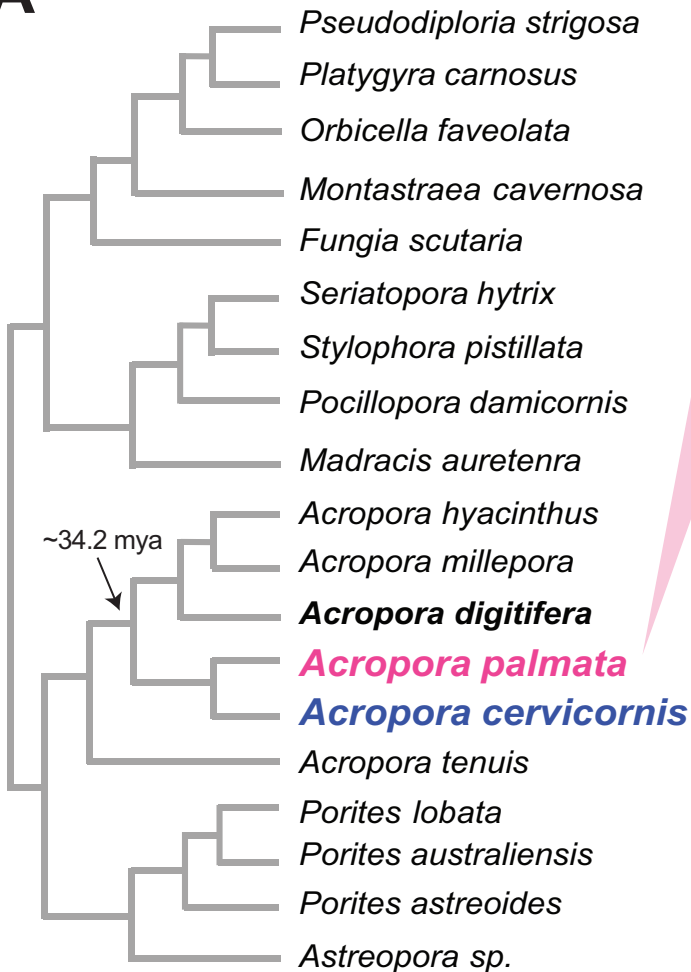
940 **Figure S8. ATP-binding cassette sub-family D member 2 alignment of several coral**
941 **sequences and human orthologue (GenBank: NP_005155.1).**

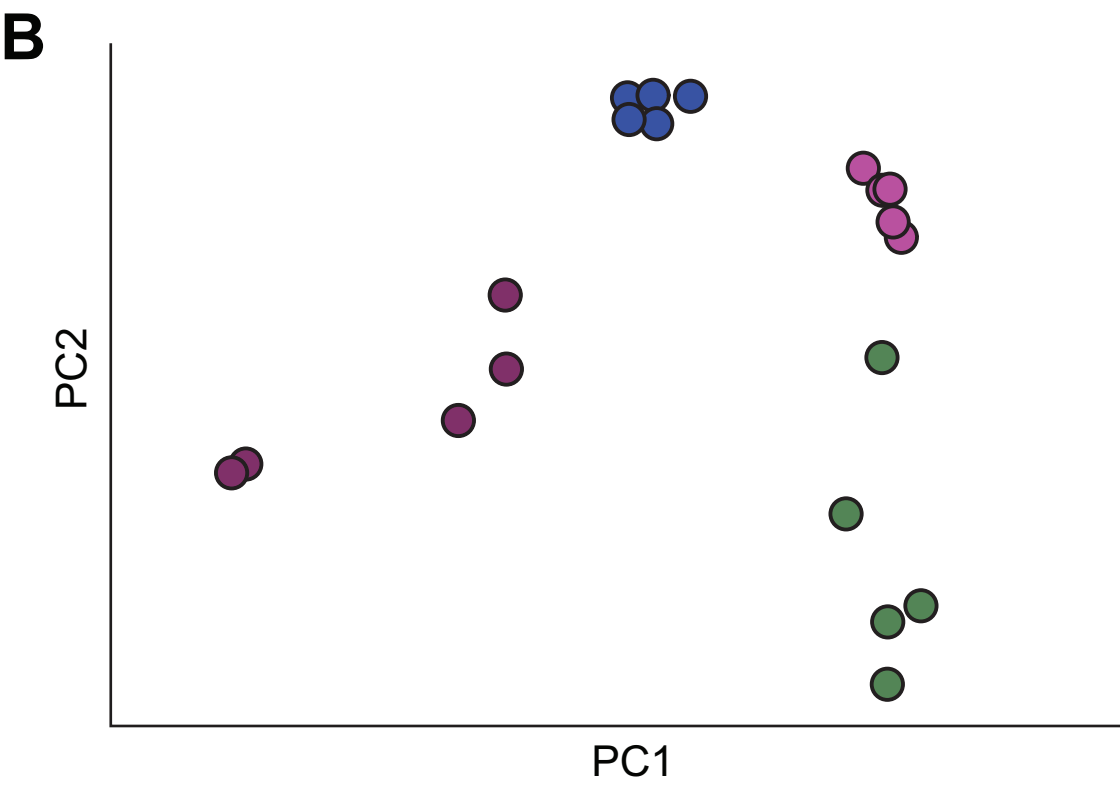
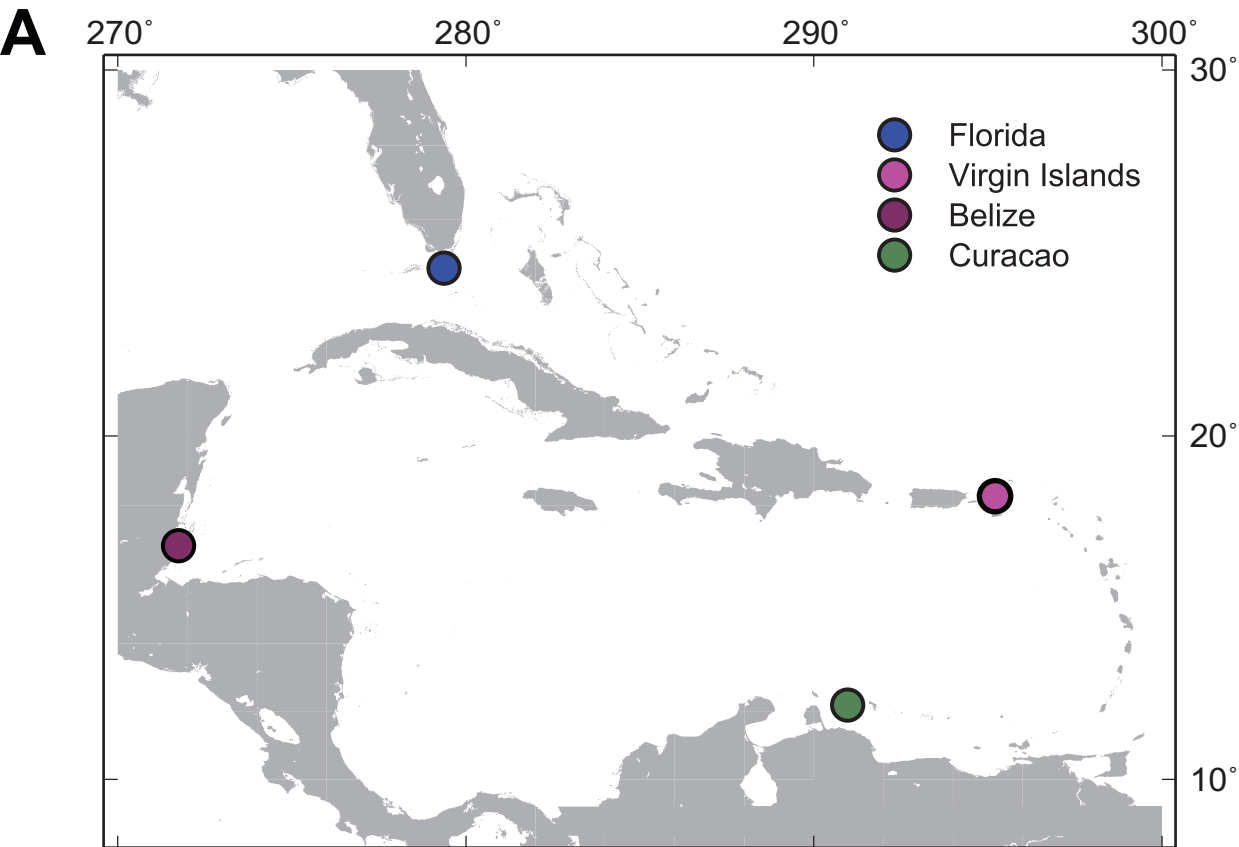
942

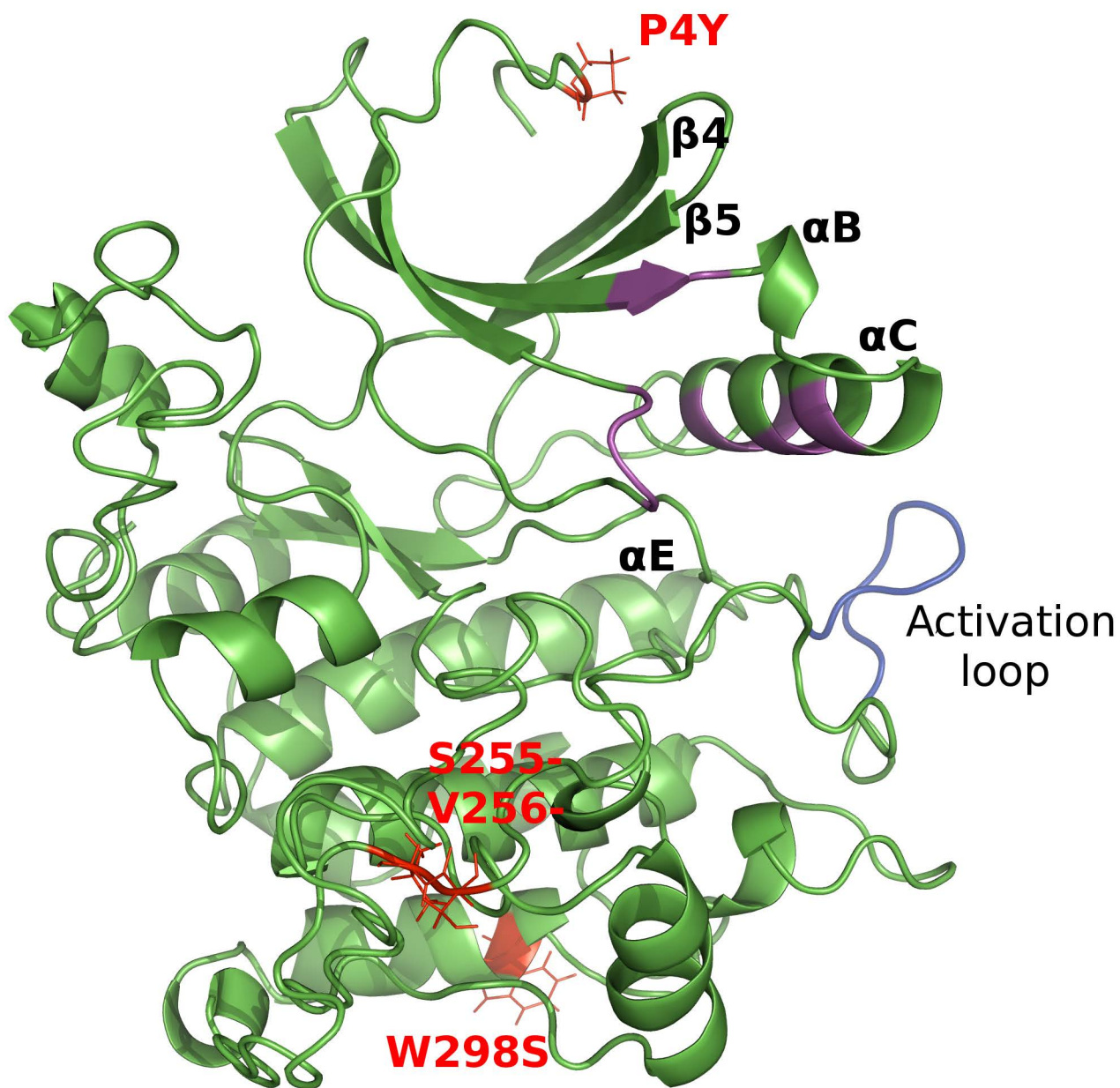
943 **Figure S9. Extreme conservation in vertebrates of the motif SVAHLYSNLTKPILDV in**
944 **ATP-binding cassette sub-family D member 2 (the human gene is transcribed right-to-left).**

945

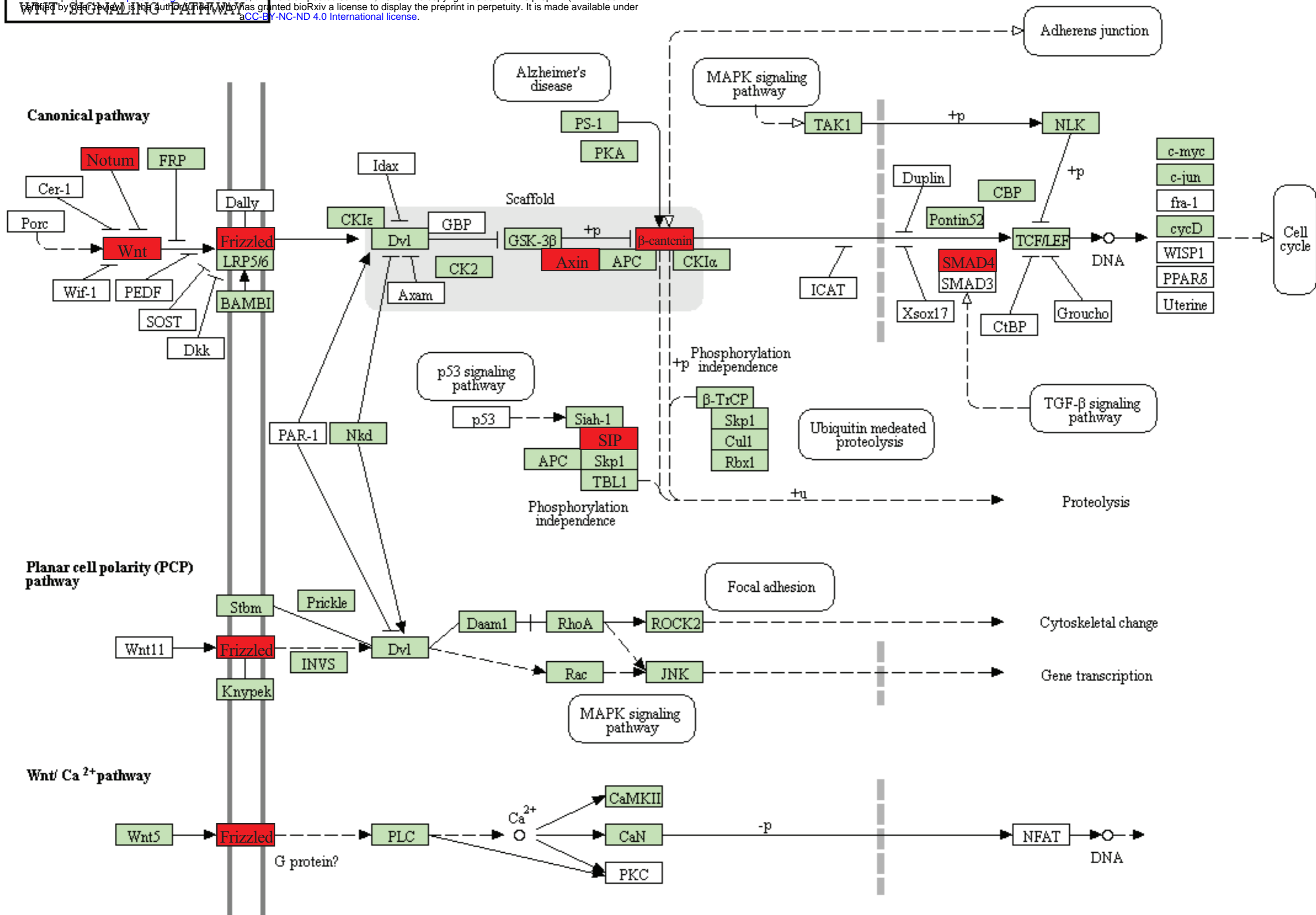
946 **Figure S10. RFLP results for parental species and hybrids for two fixed SNV loci.** The
947 restriction fragment length polymorphism results of two loci, locus NW_015441435.1: 299429
948 that cuts *A. cervicornis* (A) and locus NW_015441068.1: 984261 that cuts *A. palmata* (B), are
949 displayed in order from left to right for *A. cervicornis* genome sample 13696, *A. palmata* genome
950 sample 13815, F1 hybrid sample 8939, and three later generation (LG) hybrid samples 4062,
951 6791, and 1302. Each lane is labeled as either marker= M, uncut PCR product = U, or cut PCR
952 product = C. The LG hybrid 1302 presents both heterozygous (A) and homozygous (B) alleles,
953 whereas LG hybrid 6791 is heterozygous and 4062 is homozygous for both loci.

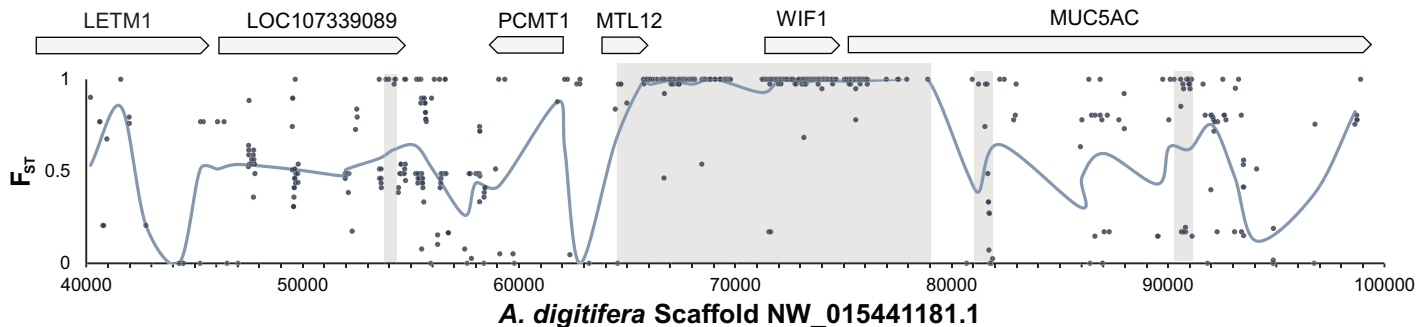
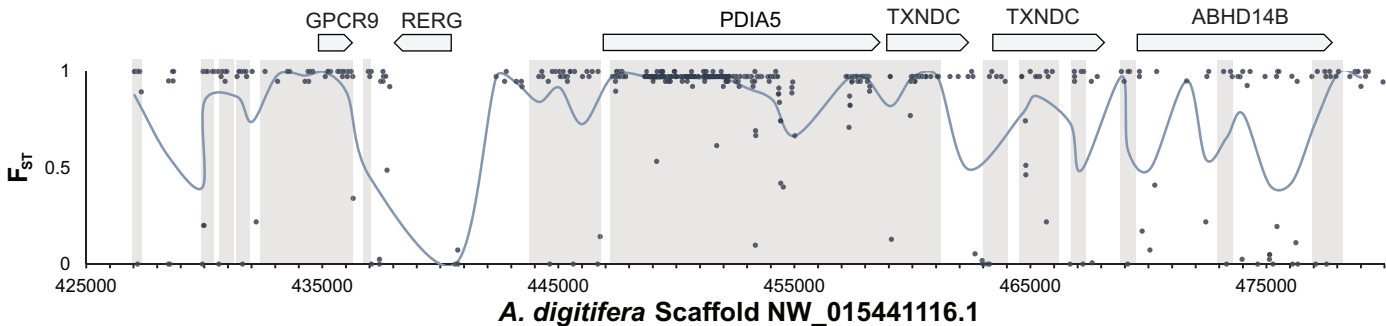
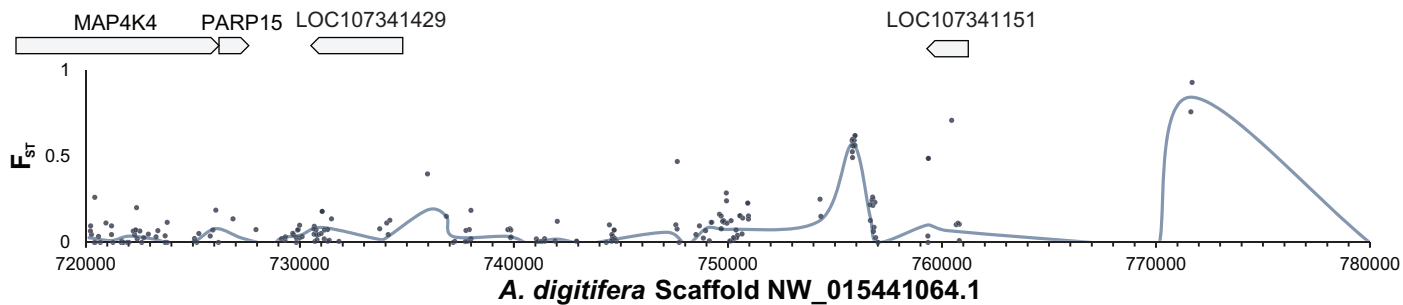
A**B****C**





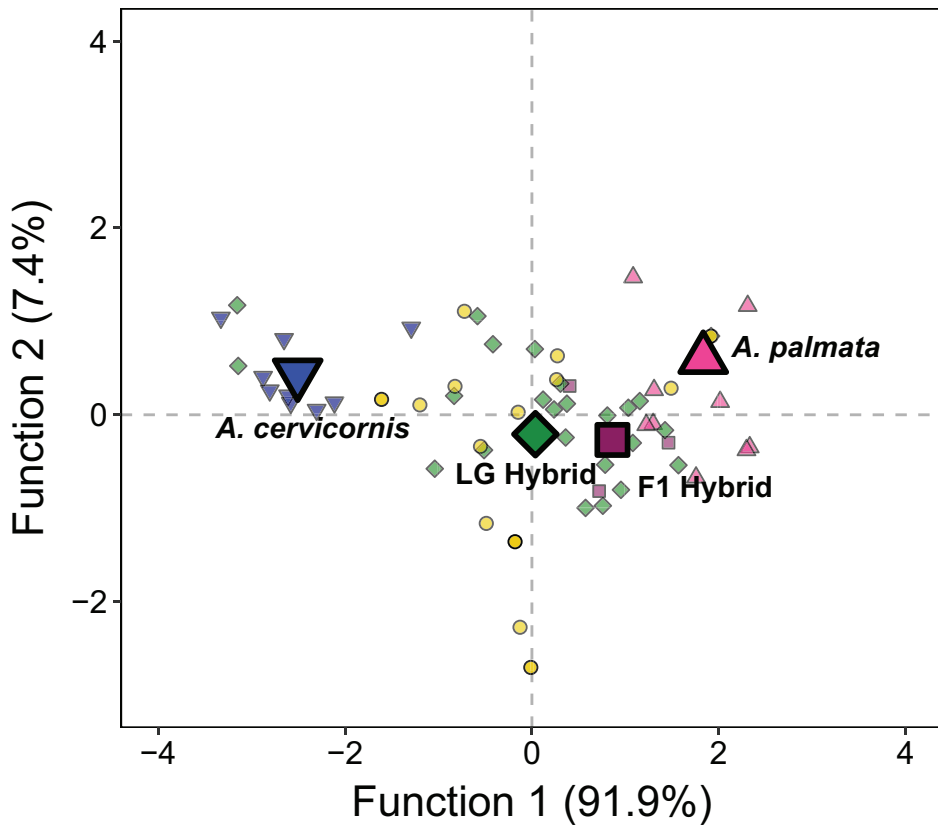
WNT SIGNALING PATHWAYS



A**B****C**

A

▼ C ■ F1 ◆ H ▲ P ● T

**B**

▼ C ■ F1 ◆ H ▲ P ● T

